FMRP DEPENDENT SYNAPTIC DELIVERY OF MESSENGER RNA

BY

DER-I KAO

DISSERTATION

Submitted in partial fulfillment of the requirements
for the degree of Doctor of Philosophy in Cell and Developmental Biology
in the Graduate College of the
University of Illinois at Urbana-Champaign, 2010

Urbana, Illinois

Doctoral Committee:

Professor Jie Chen, Chair
Associate Professor Charles L Cox, Director of Research
Professor William T Greenough, Director of Research
Associate Professor Philip A Newmark
Associate Professor Stephanie Ceman

Abstract

Fragile X mental retardation is the most common inherited form of mental retardation. The loss of FMRP function results in Fragile X Mental Retardation. In this dissertation, I investigated the regulatory role of FMRP involved in synaptic mRNA delivery.

In chapter 1, the molecular mechanism of local protein synthesis and synaptic mRNA delivery and its roles in Fragile X syndrome and learning and memory are introduced. In chapter 2, my data demonstrated that FMRP can facilitate mRNA deceleration and localization in dendritic spines upon neurotransmitter stimulation. Consistent with these findings, local protein synthesis was also enhanced in dendritic spines after stimulation. These results suggested that FMRP could mediate synaptic mRNA delivery for local protein synthesis. In Chapter 3, the role of FMRP splicing isoforms in synaptic mRNA delivery was investigated. My data suggested phosphorylation regulation and multiple isoforms of FMRP will be required to restore mRNA targeting to dendritic spines.

In conclusion, synaptic mRNA delivery regulated by FMRP isoforms was demonstrated as a novel mechanism underlying altered cognitive deficits associated with Fragile X Syndrome. When mRNA cannot be targeted properly for translation, it may result in deficits in spine structure and neurological phenotypes, such as Fragile X Syndrome. My research also corroborates the importance of spatial accuracy of protein synthesis at a microscopic level in the nervous system.

This dissertation is dedicated to my grandparents, dad, sister and my fiancé, who have offered unconditional support and understanding during the pursuit of my PhD degree.

Acknowledgements

I am heartily thankful to my advisors, Bill and Ivan Jeanne, who have provided endless scientific guidance, support and encouragement throughout my PhD studies, allowing me to develop independent research skills and pursue my scientific curiosity to accomplish my projects. I am deeply grateful to Lee's kind help and insightful advice to guide me to finish my dissertation work. I also would like to acknowledge my committee members for their great input and guidance, helping me to adjust my research direction. Greg gave me great advice on scientific writing and presentation. Georgina shared her knowledge and assisted me to accomplish the work on YFP spines. Deepa always gave great suggestions during lab meeting. Also, I want to thank other Greenough lab members, Beckman animal facility staffs, Shiv and Glenn in IGB and members of the Galvez lab, Cox lab, Clayton lab, Feng lab, and Sweedler lab for their true friendship and generosity in sharing techniques and reagents. I could have not accomplished my work without any of them.

Table of contents

Chapter 1.

Background

Fragile X Syndrome.

Fragile X Syndrome (FXS) is the most common form of inherited mental retardation and is caused by the loss of function of the *FMR1* gene, which encodes fragile X mental retardation protein (FMRP) [1]. FXS affects 1 in 4000 males and 1 in 6000 females on average and is characterized by hyperactivity, attention deficits, autistic like behaviors, seizures, and in males macroorchidism [2]. The molecular basis of fragile X syndrome has been determined. The expansion of CGG repeats (230 to more than 1000 copies) in Fragile X individuals results in the concomitant methylation of the putative CpG island promoter region located 250bp upstream with subsequent abolition of FMR1 transcription [3-5]. The absence of *FMR-1* mRNA and consequent FMRP expression is the cause for the disorder since FMRP expression is highly enriched in the normal brain and testis, which are relevant to the clinical phenotype [6].

Mental impairment related phenotypes in Fragile X Syndrome have been studied extensively since the *fmr1* knockout mouse model was generated [7]. Dendritic spine morphology in the cerebral cortex of FXS patients and in the *fmr1* KO mouse model shows more immature long thin spines than mature stubby, mushroom-shaped spines during development [8]. Interestingly, spine morphology is also altered in other genetic disorders causing mental retardation, such as Down syndrome [9]. Furthermore, group I-metabotropic glutamate receptor (mGluR) dependent long term depression (LTD) in the hippocampus is exaggerated in the *fmr1* KO model and this has been shown to be associated with glutamate receptor subunit, GluR1, internalization [10]. These findings suggest that FMRP functions in synaptic development and plasticity.

Protein synthesis dependent synaptic plasticity in neurons.

Local protein synthesis at synapses is the mechanism to provide synapse-dependent changes localized to the stimulation source. Neurons have a highly polarized cell structure and typically one long axon and multiple dendrites. Dendrites differ from axons morphologically and functionally. The synapse is the specialized structure that allows communicating between two neurons. Their communication is both through chemicals (neurotransmitters) and through electrical current. The pre-synaptic compartment contains synaptic vesicles filled with neurotransmitter, which are ready to release into the synaptic cleft when the membrane is depolarized by an action potential. Subsequently, both ionotropic and metabotropic neurotransmitter receptors on the post-synaptic compartment, closely apposing to the presynaptic compartment, are activated by neurotransmitters. The activation of these receptors can cause protein synthesis or post-translational modification in the post-synaptic compartment to modify the molecular contents for synaptic plasticity establishment or maintenance. Persistent, activity-dependent changes at individual synapses are a mechanism, termed synaptic plasticity, by which the brain encodes and stores information. Synaptic plasticity can also involve the alteration of electrophysiological and structural properties of a synapse. Previous studies have shown that activity-dependent local translation is a fundamental mechanism underlying synaptic plasticity [11, 12]. Inhibition of protein synthesis attenuates specific types of synaptic plasticity and learning behaviors [13-16]. Strikingly, animals lacking dendritic CaMKIIα mRNA and protein had reduced long-term potentiation (LTP) and impaired memory performance [17]. Morphological changes in dendritic spines can also be blocked by protein synthesis inhibitors [18]. These data suggest that local protein synthesis of dendritic mRNA at activated synapses is critical to maintain synaptic function and structure underlying learning and memory.

Evidence of synaptic protein synthesis.

The regulation of polyribosome and mRNA delivery to synapses is the key determinant to produce specific protein in a single synapse to modify local synaptic strength. Early studies found that polyribosomes and certain mRNA are identified in dendritic

compartment in addition to the neuronal cell body [19-21]. By using electron microscopy, Steward et al. found that most synapses have closely associated polyribosomes during periods of maximal synaptogenesis, implying that local protein synthesis is very important during periods of synapse growth [22]. Interestingly, the thickness of the postsynaptic density in the sensorimotor area is positively correlated with the number of ribosomal inclusions [23]. Following synaptic stimulation leading to LTP in the CA1 region of the hippocampus, polyribosomes appear to relocate from the base of the spine into the spine head [24]. The data suggest that synaptic localization of polyribosomes is regulated by neuronal activity and highly correlates with positions of increased translational capacity.

Dendritic mRNAs have been identified by *in situ* hybridization and biochemical isolation of synaptoneurosomes or synaptodendrosomes, which are the subcellular fractions enriched with axon and postsynaptic connections [21]. Since dendritic localization in the hippocampus and the cerebellar cortex can be recognized by distinct neuropil layers that contain dendrites but few neuronal cell bodies, in situ hybridization on tissue sections provide good spatial orientation to identify dendritic mRNAs. Dendritic localization of MAP2 [25], CaMKIIα [26], Arc/Arg3.1 [27] and other mRNAs were identified by using *in situ* hybridization. For biochemical approaches, FMRP [12] and CaMKIIα [28] were identified in synaptoneurosomes to be translated in response to glutamate receptors (NMDA or group I mGluR) activation. The pool of dendritic mRNAs encodes a multitude of synaptic proteins: scaffolding proteins (such as PSD-95), protein kinases (such as CaMKIIα), receptors (such as GluR1, one subunit of AMPA receptor), cytoskeleton associating proteins (such as MAP2), transcription factors (such as CREB), and others [29]. The evidence further corroborates the presence of selective mRNAs in neuronal dendrites as well as synapses.

Protein synthesis present in local compartments was established in synaptoneurosomes and isolated dendrites. Weiler et al. demonstrated a rapid polysome-association pattern of *Fmr1* mRNA and production of FMRP in synaptoneurosomes after group I mGluR stimulation [12]. Local incorporation of radio-labeled amino acid was also demonstrated in physically isolated dendrites [30]. In two independent studies using visually isolated

dendrites, authors showed that there are protein synthesis hotspots in close proximity of ribosomes following group I mGluR or BDNF activation [31, 32]. In a higher resolution experiment using electron microscopy, Krichevsky et al. elegantly demonstrated that depolarization reorganizes biochemically isolated mRNA granules and induces a less compact structure of their ribosomes [33]. Therefore, protein synthesis and the association between polyribosome and mRNA are tightly regulated by neuronal activity.

Molecular machinery of dendritic mRNA transport.

The coordinate mechanism of RNA localization and local translation has been extensively studied as it allows spatio-temporal modulation of local protein repertoires. In *Xenopus* oocytes, Vg1, a member of the transforming growth factor-β family involved in mesoderm induction, can only be translated subsequent to the localization of its mRNA to the vegetal pole [34]. Elevated gradient of Nanos protein in the posterior pole of the Drosophila embryo establishes antero-posterior patterning. This gradient results from both *nanos* mRNA translational repression in the bulk of the embryo and translational activation of *nanos* mRNA localized at the posterior pole [35]. RNA transport is particularly important to neurons due to the complexity of their intracellular compartments and the use of local translation in these compartments for focal regulation of development and synaptic strength [36]. Localized mRNAs are transported in large ribonucleoprotein complex particles (RNPs), which have been referred as RNA granules. Neuronal RNA granules often contain specific RNA binding proteins, mRNAs, adaptors connecting RNA binding proteins and motor proteins, and motor proteins despite diversity of composition and function among granules [37].

The molecular content and involvement in local mRNA translation of neuronal RNA granules have been intriguing in neuroscience field. Neuronal RNA granules originate in the nucleus because of the presence of hnRNPs, splicing components, exon-junction complex (EJC) proteins and other nuclear proteins [36]. Functionally, splicing events could be regulated and occur in distal dendrites in order for alternate splicing variants to be translated [38, 39]. Moreover, nonsense-mediated decay (NMD) can be carried out in

neuronal dendrites to restrict spatial and temporal protein expression [40]. The transport of mRNA is tightly coupled to the repression of translation at the step of translation initiation or elongation. Sossin et al. [36] defined RNA transport particles as the transport complex containing no ribosomes. In RNA transport particles, mRNAs have no access to ribosome until they are released from the complex. Therefore, translation of mRNAs in transport particles is repressed in the initiation stage. On the other hand, some RNA granules contain large and small ribosomal subunits. Translation is also repressed in these structures but at the elongation stage. As described in Krichevsky et al, by using electron microscopy they identified RNA granules as a macromolecular structure, which are highly enriched in Staufen (an RNA binding protein) and contain densely packed clusters of ribosomes. Depolarization reorganizes granules and induces a less compact organization of their ribosomes [33]. The reorganization process in response to depolarization suggests that mRNA and ribosomes are released from highly compact repression structures and become accessible to each other, and then translationally active. Interestingly, while expression of phosphorylated FMRP on serine 499 leads to an increase in stalled polyribosomes, non-phosphorylated FMRP loses the ability, suggesting that its dephosphorylation may lead to the release of polyribosomes from the stalled state [41]. The data suggests that FMRP could be involved in the transition between translation repression and de-repression.

Protein components of neuronal RNA granules have also been investigated systematically. Kanai et al [42] isolated a RNase-sensitive granule (1000S~) as a binding partner of KIF5 (kinesin heavy chain). After analysis by 2D-gel and MS/MS, the granule contains 42 proteins including those for RNA transport (such as FMRP, Pur and Staufen), protein synthesis (such as EF-1α and eIF2α), RNA helicase, and other RNA associated functions. In a proteomics study, RNA granule enriched fraction was also purified from rat embryonic day 18 brains. Abundant protein components of this fraction are determined by tandem mass spectrometry. Although the isolated proteins are not exactly the same as those identified in Kanai et al, they also include ribosomal proteins, RNA-binding proteins, and motor proteins [43]. These studies provide a broader view of RNA granule components and their implication in RNA transport and delivery.

Synaptic targeting of mRNAs.

Enduring synaptic modification requires the selective delivery of new mRNA transcripts to the synapses that are to be modified. Synaptic targeting of *Arc* (activity-regulated cytoskeleton-associated protein) mRNA is the best-studied synaptic delivery model to date. Steward et al. [44] elegantly presented that high frequency activation of the afferent perforant path projections to the dentate gyrus results in newly synthesized *Arc* mRNA to selectively localized in activated dendritic segments. At the same time, Arc protein also accumulates in the portion of the dendrite that had been synaptically activated. By applying local pharmaceutical treatment, it is further confirmed that synaptic targeting of *Arc* mRNA requires NMDA receptor activation, ERK phosphorylation and actin polymerization [45, 46]. It suggests that signaling network and actin organization are critical to localize and anchor mRNA to activated synapses. This series of studies shed light on the physiological significance of synaptic targeting of selective mRNAs.

Dendritic spines, where actin is the major cytoskeletal elements, are the specialized structure of excitatory synapses. There are other studies using dendritic spines as local synaptic targets of mRNA docking after excitatory stimulation. TLS (translocated in liposarcoma)-containing mRNP complexes can associate with myosinVα and be targeted to spines following group I mGluR activation. In the presence of a dominant negative form of myosinVα, the TLS complex failed to be translocated into spines [47]. Interestingly, following group I mGluR stimulation, FMRP-containing mRNP complex could move into spines as shown by colocalization with PSD-95 and Shank proteins [48]. However, because PSD-95 and Shank could also appear in the dendritic shaft, the localization of FMRP containing mRNP complex in dendritic spines needs to be further characterized. Polyribosomes also relocate to dendritic spines in response to tenatic stimulation [24, 49], although they preferentially localize under the base of dendritic spines before stimulation [50]. In summary, these previous studies suggest that both ribosomes and mRNAs can be delivered to dendritic spines. The process of synaptic mRNA docking is possibly mediated by coordinating RNA transport granules dynamics, mRNA association with myosin motor proteins, and activation of actin organization.

Local protein synthesis regulated by FMRP.

FMRP is a ribosome-associated protein also with selective affinity to mRNAs [51-54]. Local production of specific proteins is critical for enduring synaptic modification. For instance in the *fmr1* KO model, it has been shown that aberrant synthesis of individual proteins such as CaMKIIα, PSD-95 and MAP1b, following group 1 mGluR stimulation, is associated with defective long-term synaptic plasticity [55-57]. Additionally, AMPA receptor internalization, necessary for regulating synaptic strength, is also affected by the dysregulated protein synthesis in *fmr1* KO neurons [14, 58, 59]. Emerging evidence indicates that RNA binding proteins, ribosomes, translation factors and mRNAs encoding proteins critical to synaptic structure and function localize to neuronal processes [42]. FMRP, mRNA and other RNA binding proteins can form RNP (ribonucleoprotein) or granule structures and couple with motor proteins to be transported in dendrites [42, 60, 61]. RNAs are transported into dendrites in a translationally quiescent state where translation mechanisms are activated by synaptic stimuli [62-64]. Dendritic transport of FMRP and associated mRNAs, such as *Fmr1*, CaMKIIα, and MAP1b, are regulated by group I mGluR signaling [63, 65]. However, it is not yet fully understood how and when mRNA is delivered to the synapse and translated. Local delivery of mRNA to active synapses could provide a high degree of regulation and flexibility of protein synthesis [24, 31, 32, 50, 66]. The molecular mechanism of FMRP mediated mRNA delivery implicated in synaptic plasticity is investigated in this thesis.

FMRP associated mRNAs.

FMRP is identified as an RNA binding protein containing two KH domains, first described in hnRNP K protein, and one RGG box, an arginine- glycine- rich region found in a variety of nuclear and nucleolar proteins [67]. The identity and function of mRNAs associating with FMRP has attracted major interest in the field. *Fmr1* mRNA is the first reported FMRP associated mRNA with strong affinity to FMRP [51]. Later in 2001, there were two microarray articles reporting the pool of mRNA associated with FMRP. Miyashiro et al [53] developed antibody-positioned RNA amplification (APRA), to identify the RNA cargoes associated with the *in vivo* configured FMRP messenger

ribonucleoprotein (mRNP) complex in intact neurons. Among all RNA candidates, RGS5, DAG1 (dystroglycan associated glycoprotein 1) and GRα (glucocorticoid receptor α) show different subcellular distribution in the Purkinje neurons of *fmr1* KO cerebellum than in wild type. In later independent studies, the regulatory role of FMRP in RGS5, $GABA_A$ receptor-δ subunit [65] and Rab3a [68] was further confirmed. Brown et al [54] utilized immunoprecipitation to identify mRNAs in FMRP-mRNP complexes. The association between MAP1b [57], SAPAP4 [65] and semaphorin 3F [69, 70] and FMRP was further confirmed by later studies. From both results, a large number of candidate genes encoding cell signaling molecules, cytoskeleton/cell structure components and receptor subunit were retrieved. It suggests that the lack of FMRP in Fragile X Syndrome patients can lead to dysregulated synaptic expression of its many associated mRNAs, which could account for subsequent plasticity deficits. However, there is no overlap of RNA candidates between these two studies and *Fmr1* mRNA was not identified. Therefore, more systematic studies are still ongoing in other labs.

There are also a lot of studies focusing on investigating FMRP-associated mRNAs and their roles in synaptic plasticity. Ca^{2+}/calmodulin-dependent protein kinase II subunit α (CaMKIIα), in a calcium and calmodulin dependent manner, phosphorylates many different brain substrates including synapsin I, tyrosine hydroxylase and nitric oxide synthase. Therefore, CaMKIIα is able to perform regulatory functions associated with increases in intracellular free calcium. Its activity is also involved in modulating AMPA and NMDA receptor-mediated synaptic transmission [71]. CaMKIIα is highly enriched in the postsynaptic density of hippocampus and neocortex [72] and its protein level is elevated upon synaptic stimulation [28, 73]. By using genetic models, it has been shown that CaMKIIα is involved in both long-term potentiation (LTP) and long-term depression (LTD) events depending on stimulation paradigm and brain regions [74, 75]. FMRP can regulate CaMKIIα protein levels following group I mGluR stimulation [55]. In *fmr1* KO neurons, dendritic transport of CaMKIIα mRNA in response to stimulation is impaired [65]. Therefore, in the absence of FMRP, CaMKIIα protein cannot be expressed properly to carry out its kinase activity for subsequent synaptic events.

PSD-95 (postsynaptic density protein 95) is a scaffolding protein containing PDZ domains that provide association with receptors and cytoskeletal elements at synapses. PSD-95 is also involved in maturation of excitatory synapses [76]. It has been shown that FMRP regulates PSD-95 protein synthesis by mediating PSD-95 mRNA association with polyribosomes at synapses [56, 64]. The evidence suggests that in the absence of FMRP in Fragile X syndrome, PSD-95 mRNA cannot associate with polyribosomes or be translated efficiently for the maintenance of the structure of excitatory synapses.

MAP1b (microtubule-associated protein 1b) controls neurite extension and growth cone motility via modulating microtubule dynamics [77]. MAP1b may be also involved in group I mGluR induced AMPA receptor endocytosis to alter synaptic strength [78]. In *fmr1* KO neurons, the aberrant MAP1b expression during development leads to abnormally increased microtubule stability [57]. FMRP is able to associate with MAP1b mRNA and regulate its dendritic transport [65, 79]. These results suggest that FMRP controls MAP1b translation to modulate the dynamic organization of neuronal cytoskeleton and synaptic connections, and the abnormal microtubule stability caused by FMRP deficiency could contribute to the impaired synaptic maturation in Fragile X Syndrome.

FMRP isoforms.

FMR1 pre-mRNA has four alternative splicing sites and can give rise to as many as 24 different mRNAs and to 24 possible corresponding proteins (Figure 1.1) [80-82]. The functions carried out by individual FMRP isoforms or by their interaction are poorly understood because the majority of our knowledge regarding Fragile X Syndrome is based on *fmr1* knockout model, in which all isoforms are missing. Therefore, it could be of important clinical relevance to understand if different isoforms are associated with distinct functions. To also better assess the possibility of gene therapy for Fragile X Syndrome, we have to understand FMRP isoform functions in greater detail. The first alternative spicing site of *Fmr1* around exon12 creates iso-1, including exon12, and iso-7, lacking exon12 (Figure 1.1). The second alternative spicing site utilizes three alternative

splice acceptor sites on exon15 (ex15a, ex15b, or ex15c) with exon14 included or excluded to produce 6 splicing variants (Figure 1.1). The predicted mRNA including exon14 are referred as *Fmr1* iso-2 (alternate acceptor b, exon15b) and *Fmr1* iso-3 (alternate acceptor c, exon15c), and the corresponding isoforms lacking exon12 would be referred to as *Fmr1* iso-8 and iso-9. Similarly, exon14 is spliced out on iso-4, 5, 6, 10, 11, and 12. The exclusion of exon14 from *Fmr1* message causes the loss of nuclear export signal (NES) and a +1 frame shift in the *Fmr1* reading frame downstream of the splicing site. Since the *Fmr1* isoforms lacking exon14 will be restricted inside the nucleus [83], their dendritic localization and function will not be studied here. The last alternative splicing occurs to include or exclude a 5' fragment of exon17 (Figure 1.1). Because there is no important functional domain on exon17, these isoforms were poorly studied.

The diversity of FMRP isoforms containing or lacking exon12 in conjunction with using different exon15 splicing acceptors could contribute to a pool of proteins with distinct functions in neuronal dendrites. Exon12 encodes a hydrophobic loop in the KH2 domain, one of three RNA binding sites on FMRP, which has preferential affinity with kissing complex RNA [82]. Exon12 variant proteins might differentially associate with kissing complex *in vitro* [84]. Therefore, the presence or absence of exon12 could affect selective RNA binding affinity of FMRP. The exon15 splicing variants can be differentially phosphorylated and methylated and possibly result in distinct RNA binding preference [84-86]. In adult and embryonic stages, FMRP isoforms without exon12 are more abundant than those containing exon12; FMRP isoforms containing full length exon15 (Ex15a) are more abundant than other spliced forms [84]. To add to this limited information, I will examine dendritic function of four specific FMRP isoforms (Figure 1.1).

Figures

Figure 1.1 Alternative splicing of *Fmr1*.

(a) *Fmr1* exons (8-17) represented by boxes. A full length *Fmr1* mRNA (blue) is represented with corresponding functional domains (red) and alternative splicing sites (black lines). Three RNA binding domains, KH1, KH2, and RGG, nuclear export signal (NES), and phosphorylation site (S499) are indicated.

(b) *Fmr1* mRNAs of iso1-iso12 are represented. Iso1, 2 and 3 use alternative splicing acceptor of exon15 a, b, or c. Besides the variation in exon15 acceptor sites, iso7, 8 and 9 do not contain exon12. Iso4, 5, and 6 have similar exon15 splicing acceptor variations but use 5'end of exon14 as the splicing donor. Therefore, the event to splice out exon14 (containing NES) causes the protein to be restricted to the nucleus and also causes a frame shift downstream of exon14. Iso10, 11, and 12 have the same variation in exon14 and 15 as iso4, 5, and 6 but they do not contain exon12. The study of isoform function in synaptic mRNA targeting will be focused on iso1, 2, 7, and 8, as circled on the diagram.

a.

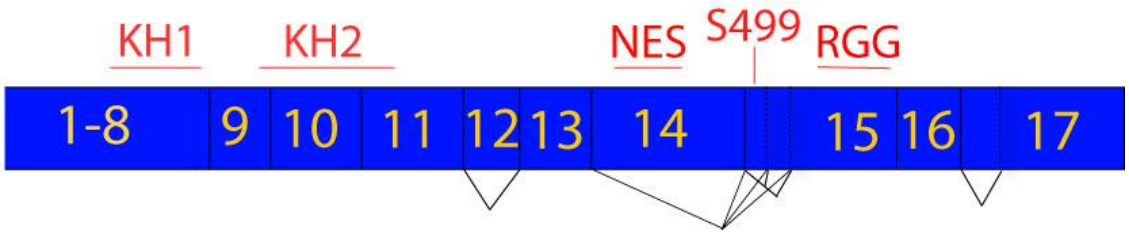

Figure 1.1 Alternative splicing of *Fmr1*. (cont.)

b.

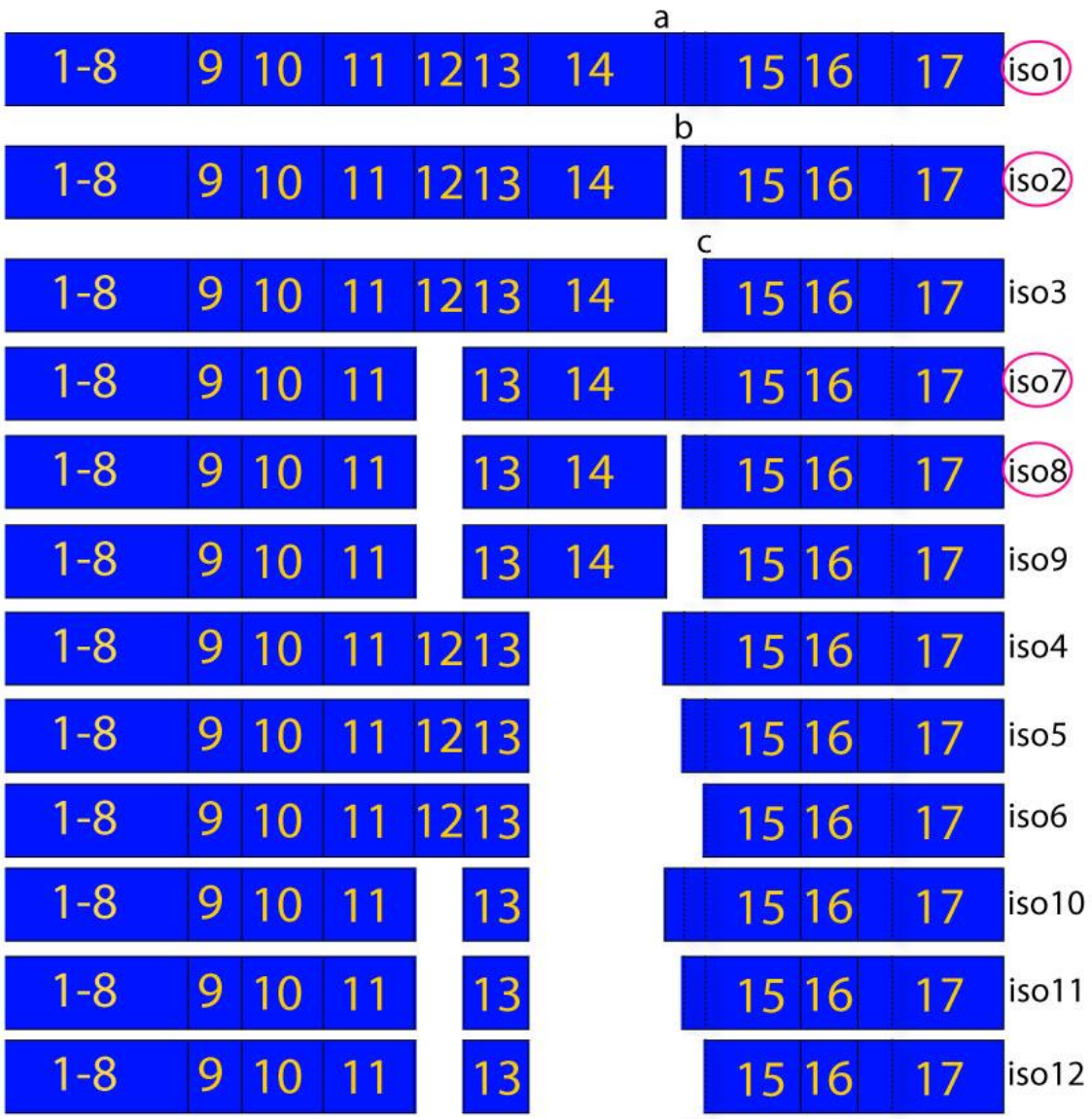

Chapter 2.

Altered mRNA transport, docking, and protein translation in neurons lacking fragile X mental retardation protein

(Data presented here were originally published in *Proc Natl Acad Sci U S A. 2010 Aug 31; 107(35):15601-6.*)

Abstract

Fragile X syndrome is caused by the absence of functional fragile X mental retardation protein (FMRP), an RNA binding protein. The molecular mechanism of aberrant protein synthesis in *fmr1* KO mice is closely associated with the role of FMRP in mRNA transport, delivery, and local protein synthesis. We show that GFP labeled *Fmr1* and CaMKIIα mRNAs undergo decelerated motion at 0-40 minutes after group I mGluR stimulation, and later recover at 40-60 minutes. Based on this finding, we investigate targeting of mRNA associating with FMRP after neuronal stimulation. We find that FMRP is synthesized closely adjacent to stimulated mGluR5 receptors. Moreover, in WT neurons, CaMKIIα mRNA can be delivered and translated in dendritic spines at early time points in response to group I mGluR stimulation, whereas KO neurons fail to show this response. Lastly, GluR1 internalization occurs after stimulation in spines of WT neurons but instead is constitutively internalized in the dendrites of *fmr1* KO neurons. These data suggest that FMRP can mediate spatial mRNA delivery for local protein synthesis to establish plasticity in response to synaptic stimulation.

Introduction

Fragile X syndrome (FXS) is the most common form of inherited mental retardation and is caused by the loss of function of the *FMR1* gene, which encodes fragile X mental retardation protein (FMRP) [1]. FXS affects 1 in 4000 males and 1 in 6000 females on average and is characterized by hyperactivity, attention deficits, autistic like behaviors,

and seizures [2]. Dendritic spine morphology in the cerebral cortex of FXS patients and in the *fmr1* KO mouse model shows more immature long thin spines than mature stubby, mushroom-shaped spines [8]. Furthermore, group I-mGluR dependent long term depression (LTD) in the hippocampus is exaggerated in the *fmr1* KO model and this has been shown to be associated with GluR1 internalization [10]. These findings suggest that FMRP functions in synaptic development and plasticity.

Activity-dependent local translation is a fundamental mechanism underlying synaptic plasticity [11, 12]. Inhibition of protein synthesis attenuates specific types of long-term plasticity [13, 14]. Morphological changes in dendritic spines can also be blocked by protein synthesis inhibitors [18]. Local production of specific proteins is critical for enduring synaptic modification: for instance in the *fmr1* KO model, it has been shown that aberrant synthesis of individual proteins such as CaMKIIα, PSD-95 and MAP1b, upon group 1 mGluR stimulation, is associated with defective long-term plasticity [55-57]. Additionally, AMPA receptor internalization, necessary for regulating synaptic strength, is also affected by the dysregulated protein synthesis in *fmr1* KO neurons [14, 58, 59]. Here, we have studied specific molecular mechanisms that may elucidate aberrant translation in the *fmr1* KO model.

The molecular basis of FMRP's role in translation dependent plasticity remains unclear despite extensive study. FMRP is a ribosome-associated RNA binding protein with selective affinity [51-54]. Upon neuronal stimulation, FMRP may regulate protein levels by mediating translational regulation and mRNA trafficking [63, 64]. FMRP, mRNA and other RNA binding proteins can form RNP (ribonucleoprotein) or granule structures and couple with motor proteins to be transported in dendrites [42, 60, 61]. Dendritic transport of FMRP and associated mRNAs, such as *Fmr1*, CaMKIIα, and MAP1b, are regulated by group I mGluR signaling [63, 65]. Studies have shown that *Arc* mRNA can be targeted to active synapses upon high frequency stimulation in the perforant pathway [44, 87]. However, it is not yet fully understood how and when mRNA is delivered to the synapse and translated. Local delivery of mRNA to active synapses could provide a high degree of regulation and flexibility of protein synthesis [24, 31, 32, 50, 66].

We hypothesized that FMRP regulates dendritic mRNA dynamic motions leading to local protein synthesis and subsequent plasticity in response to neuronal stimulation. We investigated the speed and directionality of mRNA movement upon group I mGluR stimulation using time-lapse imaging of cultured WT and *fmr1* KO neurons. We found that at 0-40 minutes after stimulation the speed of mRNA containing granules showed a reduction in WT but not KO dendrites, and at 40-60 minutes mRNAs resumed more directional motion. In the early time points after stimulation, FMRP was also translated in regions closely adjacent to mGluR5. CaMKIIα mRNAs and proteins were more enriched at dendritic spines in WT, but not *fmr1* KO neurons. Interestingly, we showed GluR1 internalization occurred at spines after stimulation in WT neurons but remained constitutively internalized in the dendrites of KO neurons. This suggests the lack of local translation regulation and translation-dependent plasticity in *fmr1* KO neurons could originate from the aberrant mRNA targeting function in the absence of FMRP.

Materials and Methods

DNA constructs.

The GFP-MS2-nls and MS2 binding site-CaMKIIα 3'UTR constructs were kindly provided by Dr. Kenneth S. Kosik, UCSB. MS2bs vector was generated from MS2bs-CaMKIIα 3'UTR by removing CaMKIIα 3'UTR using BglII and NotI. MS2bs-*Fmr1* was constructed by insertion of the *Fmr1* ORF (open reading frame) and 3'UTR (untranslated region) PCR fragment into an MS2bs vector. The *Fmr1* fragment was generated from Mc2.17 by PCR and digestion with BamHI and NotI. All plasmids were sequenced to verify their composition.

Primary hippocampal neuron culture and transfection.

Primary neurons were prepared from hippocampi of WT or *fmr1* KO C57BL/6 mice at postnatal day 1 to 2 and maintained in Neurobasal medium supplemented with B27 and Glutamine (Invitrogen). Neurons were transfected using Lipofectamine LTX (Invitrogen). All studies were performed in compliance with the Institutional Animal Care and Use Committee of University of Illinois at Urbana-Champaign.

Time lapse imaging.

Primary WT or *fmr1* KO hippocampal neurons were transfected and imaged within 24 hours post-transfection. Neurons were maintained in Liebovitz's L-15 supplemented with B27 at 37^{o}C in a 5% CO2 live-cell incubation chamber and imaged using the 40X objective (NA 1.4) on a Zeiss Axiovert 200M microscope, before and after exposure to 50μM (S)-3,5-Dihydroxyphenylglycine (DHPG, Tocris), an mGluR group I agonist, for 5 minutes. Images were taken every 5 seconds for 25 frames.

Immunocytochemistry.

Primary hippocampal cells on coverslips were fixed using 4% paraformaldehyde in PBS and permeabilized with methanol. Neurons were incubated in primary antibody (diluted in 1% normal donkey serum) at 4^{o}C overnight. This was followed by incubation with species-appropriate secondary antibodies. For surface receptor staining, neurons were incubated with rabbit anti-FLAG (Sigma) at room temperature for 5 minutes to allow labeling of N terminal FLAG tagged receptor and washed in Neurobasal medium and PBS. After stimulation, neurons were permeabilized and examined by regular immunocytochemistry procedures.

Colocalization between FMRP and surface receptor.

Primary hippocampal neurons were transfected with FLAG-mGluR1a, FLAG-mGluR5 or FLAG-β2AR, which were kindly provided by Dr Stephan Ferguson, at 7 or 8 DIV. Cultured neurons were treated with DHPG for 5 minutes and left for the indicated duration after DHPG was removed. In cycloheximide treatment groups, cycloheximide was included in medium 30 minutes before and during experiment periods. Then neurons were subjected to surface receptor labeling and immunocytochemistry. Images were taken by Leica SP2 with a 63X (NA1.4) objective as Z-stacks with 0.3μm interval.

Fluorescence in situ hybridization.

Digoxigenin (DIG) labeled riboprobes were generated from plasmids with T3 or T7 RNA polymerase sites. A cRNA probe to CaMKIIα was generated from a restriction digested fragment corresponding to nucleotides 1014-1332 of CaMKIIα cDNA. The plasmid pBS-CaMKIIα was kindly provided by Dr. Oswald Steward, UC Irvine [88]. A cRNA

probe to *Fmr1* was generated from a restriction digested fragment corresponding to nucleotide 263-313 of *Fmr1* cDNA. The *fmr1* cDNA fragment was kindly provided by Dr Jim Eberwine, U Penn and inserted into pBS. CaMKIIα and *Fmr1* probes were labeled by in vitro transcription of the cloned insert in the presence of digoxygen**in**-dUTP (Roche). To detect total poly-adenylated mRNA, a synthetic 50-mer nucleotide oligo-dT labeled with Cy3 at 5' end was used. Hybridization buffer: 40% formamide, 10% dextran sulfate, 1x Denhardt's solution, 4x SSC, 10mM DDT, 1mg/ml tRNA, and 1mg/ml denatured salmon sperm DNA. Primary neurons were fixed with 4% paraformaldehyde, permeabilized with methanol, and then prehybridized with hybridization buffer. Then neurons were incubated with probes in hybridization buffer overnight at 55^{o}C for CaMKIIα probes or at 42^{o}C for *Fmr1* probes or two hours at 37^{o}C for poly-dT oligos. After hybridization, cells were washed in 0.5X SSC with 50% formamide, 0.5X formamide and PBS. Cells were incubated with an HRP-linked DIG antibody (Roche) and the signal was amplified by Cy3 TSA-Plus system (PerkinElmer).

CaMKIIα protein and mRNA localization in YFP spines.

WT or *fmr1* KO neurons containing Thy1-Yellow-Fluorescent-Protein (YFP) derived from B6.Cg-Tg(Thy1-YFPH)2Jrs/J (Jax Mice) were cultured to DIV18-21, stimulated with 50μM DHPG for 5 minutes, and left for the indicated period after DHPG was removed. After fixation, neurons were subjected to immunostaining or in situ hybridization as described above. Images were taken by Zeiss LSM710 with a 63X (NA1.4) objective as Z-stacks with a 0.3μm interval. All images in a single time-series group were taken under the same acquisition parameters for relative comparisons.

GluR1 internalization assay.

Live hippocampal neurons at DIV 21-22 were labeled for 10 min at 37^{o}C with a rabbit antibody directed against the extracellular region of GluR1 (Calbiochem). After washing in conditioned medium, neurons were incubated at 37^{o}C in conditioned medium containing 100μM DHPG for 5 min. In the cycloheximide treatment group, 60μM cycloheximide was present during the entire experiment. After DHPG washout, neurons were maintained for 15 minutes before fixation in 4% paraformaldehyde and 4% sucrose. Under non-permeant condition, neurons were stained with Alexa fluor555 conjugated

anti-rabbit for 1 hr at room temperature to visualize surface receptors. Neurons were then permeabilized for 1 min in 100% methanol at -20 ^{o}C and stained with chicken anti-GFP and subsequent Cy2 conjugated anti-chicken and Cy5 conjugated anti-rabbit for 1 hr to visualize YFP and internalized GluRs. Images were acquired by Zeiss LSM710 with a 63X (NA1.4) objective as Z-stacks with 0.3μm interval. Cy5 fluorescence average intensities indicative of internalization were divided by total (Alexa fluor555+ Cy5) fluorescence intensities and standardized to control group (resting state in WT).

Imaging analysis.

For time-lapse imaging, granules consistently motile during at least two time points were analyzed. Time-lapse imaging series were analyzed by ImarisTrack software (Bitplane). Total trafficking length of motile particles was measured and divided by time as average speed. The Track Displacement is the distance between the first and last position. The Track Length is the total length of displacements within the track. The track efficacy, calculated by track displacement divided by track length, is the measurement of unidirectional movement. Colocalization between surface receptors and FMRP was quantified by Mander's coefficient of FMRP staining [89]. Mander's coefficient of FMRP= sum of colocalized (Intensity of surface receptor)*(intensity of FMRP)/ sum of intensity of FMRP in one voxel, where (intensity of surface receptor) =1 when the voxel contains surface receptor staining, otherwise (intensity of surface receptor) = 0. Manders' coefficient varies from 0 to 1, corresponding to non-overlapping images and 100% colocalization. Three dimension reconstruction and surface rendering were applied to YFP neuron images by using surface function of Imaris (Bitplane). Spine and dendrite regions of interest (ROI) were defined by YFP signals without visualizing other immunofluorescence channels. Intensity of CaMKIIα protein or mRNA was calculated as absolute intensity (pixel) per volume unit (voxel) and standardized by the value of resting state in each group.

Statistical analysis.

For mean comparisons, paired-t test, one-way or two-way ANOVA were performed. Tukey's HSD or Dunnett was carried out as post-hoc analysis as mentioned in figure

legends. In all figures, data were presented as mean ± SEM, and *p<.05, **p<.01, ***p<.001.

The sources of the antibodies are as follows: rabbit anti-mGluR5 (Millipore), rabbit anti-mGluR1a (Millipore), mouse anti-MAP2 (Sigma), rabbit anti-MAP2 (Millipore), chicken anti-MAP2 (EnCor), rabbit anti-GFP (AbCam), chicken anti-GFP (AbCam), rabbit anti-FLAG (Sigma), mouse anti-FLAG (Sigma), mouse anti-FMRP (1C3), mouse anti-CaMKIIα (Millipore), and mouse anti-PSD95 (AbCam).

Results

Study of mRNA distribution in WT and fmr1 KO hippocampal neurons by time-lapse imaging.

To test whether FMRP regulates the dynamics of dendritic mRNA movement, we used time-lapse imaging to investigate mRNA movement in primary cultures of WT and *fmr1* KO hippocampal neurons. Two mRNAs, CaMKIIα and *Fmr1*, were indirectly labeled by GFP-MS2 (*Fig. 2.1.a*), using the MS2 tethering method [90, 91], and monitored by time-lapse imaging. CaMKIIα was used here because its translation is regulated by FMRP [55] and its dendritic trafficking was studied previously [90]. *Fmr1* was chosen because of its high affinity association with FMRP [51]. Since FMRP may associate with *Fmr1* either through its G-quartet on the open reading frame (ORF) and/or the U-rich region on the 3' untranslated region (UTR) [92, 93], we made a construct containing both the ORF and the 3' UTR of *Fmr1* as the RNA of interest (*Fig. 2.1.a*) to mimic endogenous *Fmr1* mRNA. *Fig. 2.1.b* shows that the ORF of the *Fmr1* mRNA construct cannot be translated, consistent with its placement downstream of the *LacZ* gene stop codon. Although a nuclear localization signal was included in the labeling system, FMRP was not trapped in the nucleus (*Fig. 2.1.c*). *Fig. 2.2.a* shows that without a dendritic targeting signal, GFP labeled MS2 binding site (MS2bs) cannot be transported to neuronal dendrites. Both MS2-GFP labeled *Fmr1* and CaMKIIα formed punctate mRNA granules in dendrites (*Fig. 2.2.b and c*). Moreover, *Fmr1*-containing GFP labeled granules were

co-localized with *Fmr1* RNA signals as shown by fluorescence in situ hybridization (*Fig. 2.2.d*), confirming that GFP labeled granules contained *Fmr1* mRNA.

Next, to compare the dynamic movement of mRNA in WT and *fmr1* KO hippocampal neurons, either CaMKIIα or *Fmr1* labeling constructs were transfected into WT and *fmr1* KO neurons. mRNA granules in single dendrites were imaged 5 seconds per frame for 25 frames (2 minutes in total) before and after stimulation by the group I mGluR agonist, DHPG (*Fig. 2.3.a*). We found that the majority of granules was stationary, as reported before [90]. Therefore, we measured the trafficking pattern of motile granules, representing their engagement with motor proteins, in at least two time-series. The movement dynamics of CaMKIIα or *fmr1* granules were measured as average speed and as unidirectional movement efficacy, which is a measurement of the degree to which the granule travels in a single direction. In WT neurons, the average speed of *Fmr1* granules (*Fig. 2.3.b Left*) was decreased between 0 and 40 minutes after DHPG stimulation compared to the speed before stimulation. However, in *fmr1* KO neurons, average speed did not change significantly after stimulation. The average speed of CaMKIIα granules showed similar changes (*Fig. 2.3.b Right*); in WT, but not KO neurons, CaMKIIα mRNA significantly slowed during 0-40 minutes post-stimulation. This suggests FMRP may act to decelerate mRNA movement in the early phase (0-40 min) after group I mGluR treatment. The average speed of CaMKIIα (82.96 nm/sec) was comparable to a previous report [90]. Interestingly, the average speed at baseline (pre-stimulation) was significantly lower in *fmr1* KO neurons compared with WT neurons.

The directionality of *Fmr1* granules in WT neurons was significantly higher during 40 and 60 minutes after DHPG treatment (*Fig. 2.3.c Left*). There was a similar trend (not significant) for CaMKIIα granules in WT neurons compared to *fmr1* KO neurons (*Fig. 2.3.c Right*). The apparent increase in unidirectional *Fmr1* mRNA movement might indicate a regulatory interaction between FMRP and motor proteins and mRNA in response to stimulation [60, 61, 65]. It is important to note that total granule number and the percentage of motile granules were not significantly different between WT and *fmr1* KO neurons. However, the brightness of *Fmr1* granules in WT was significantly higher after DHPG treatment, but not in *fmr1* KO neurons (*Fig. 2.3.d*). This suggests that

mRNA, previously below detection and measurement levels, may be incorporated into granule structures by DHPG stimulation in WT, but not KO neurons.

FMRP was translated near group I mGluRs.

Next, we used double label immunofluorescence to examine translation of FMRP in regions near group I mGluR. We chose the cellular micro-domain of group I mGluR because it is linked to signal pathways: mGluR1a-mediated ERK phosphorylation is enriched after stimulation in the membrane fraction [94] and the ERK pathway is crucial for group I mGluR dependent plasticity [95]. N-terminal FLAG tagged mGlu1a and mGluR5, two members of the group I mGluR family, were individually expressed in primary hippocampal neurons to label surface receptor regions. Surface mGluR1a and mGluR5 were recognized by anti-FLAG under non-permeabilized conditions (*Fig. 2.5.a*). Colocalization between endogenous FMRP and the surface receptor was measured at different time points after DHPG treatment (*Fig. 2.4.a*). Our results show that colocalization between FMRP and surface mGluR5 was significantly elevated at 20 minutes after DHPG treatment (*Fig. 2.4.b*). While treated with a protein synthesis blocker, cycloheximide (CHX), there was not a greater colocalization (*Fig. 2.4.c*). This suggests that FMRP was newly synthesized in regions close to surface mGluR5 in response to group I mGluR stimulation, although some FMRP transport may still occur. There was only a slight increase in colocalization between FMRP and surface mGluR1a, and this change did not occur until 40 minutes (*Fig. 2.4.d*). The difference between mGluR5 and mGluR1a may have been caused by different representation of surface receptor constructs since surface mGluR5 staining showed better representation of endogenous mGluR5 (*Fig. 2.5.b*). Lastly, surface β2 adrenergic receptor (β2AR), another G-protein coupled receptor, was used as a negative control since it cannot be stimulated by group I mGluR agonist. DHPG stimulation caused no change in colocalization between FMRP and β2AR (*Fig. 2.4.e*). This suggests translation of FMRP could be enriched temporally within active receptor regions.

FMRP targets translation of CaMKIIα to dendritic spines.

To investigate whether mRNA and newly translated protein are localized at excitatory synaptic sites in the presence of FMRP we looked at levels of CaMKIIα mRNA and protein in dendritic spines at different time points after group I mGluR stimulation. We examined the intensity of CaMKIIα protein at spines and adjacent area of dendrites in WT and *fmr1* KO neurons that endogenously expressed YFP (*Fig. 2.6.a and b*). Based on our previous results we defined five time points from the washout after 5 minutes of treatment with DHPG. At 10 minutes in WT spines the level of CaMKIIα peaks and is significantly higher than at the pre-DHPG resting state. In KO spines, on the other hand, there is a delayed, non-significant increase above baseline at 20 minutes after DHPG treatment (*Fig. 2.6.c*). Dendrites showed the same temporal pattern of protein translation as spines, although the changes were smaller, and non-significant (*Fig. 2.6.d*). Next, we compared the levels of enrichment of CaMKIIα at individual spines with the adjacent dendrite after DHPG stimulation in WT and *fmr1* KO neurons (*Fig. 2.6.e*). The ratios were standardized to the level at resting state. In WT neurons, the spine to dendrite ratio of CaMKIIα was enriched at 20 minutes after DHPG removal compared to pre-stimulation, whereas the KO showed no significant change in ratio from baseline at any time point following stimulation. Furthermore, compared with KO, WT neurons showed higher spine to dendrite enrichment of CaMKIIα at 0, 20 and 40 minutes following stimulation.

Finally, we asked if the elevated level of CaMKIIα is caused by de novo protein synthesis after group I mGluR stimulation. After neurons were treated with cycloheximide, the increase in CaMKIIα levels seen in WT spines at 10 minutes after DHPG treatment was no longer apparent (*Fig. 2.6.f*). Similarly, the spine to dendrite enrichment ratio shows an increased trend in untreated neurons that is not present after cycloheximide treatment, such that at 20 minutes there is a significant difference between the enrichment ratios in treated vs. untreated neurons (Fig. *2.6.h*). These findings suggest that in the presence of FMRP, CaMKIIα is translated and enriched at individual spines by 20 minutes after the cessation of stimulation.

Local targeting of CaMKIIα mRNA to WT spines.

To test targeting of CaMKIIα mRNA at dendrites or spines after group I mGluR stimulation we examined CaMKIIα mRNA puncta localization in YFP-labeled WT and *fmr1* KO neurons by fluorescence in situ hybridization (*Fig. 2.7.a and b*). The total number and average intensity of RNA puncta (larger than 0.3μm), as well as the ratio of RNA puncta localized in spines to total RNA puncta was calculated for each 50μm segment of dendrite. The total number of RNA puncta within 50μm of dendrite did not change over time after stimulation in either WT or *fmr1* KO dendrites (*Fig. 2.7.c*). The intensity of total RNA puncta was rapidly and significantly elevated in WT, but not in *fmr1* KO neurons, immediately after DHPG washout (0 min), compared with pre-stimulation intensity (*Fig. 2.7.d*). More interestingly, the fraction of RNA puncta at WT spines compared to total dendritic puncta was significantly higher at 0 minutes compared to baseline (*Fig. 2.7.e*). As a control for mRNA binding specificity of FMRP, we further showed that the level of polyA mRNA does not change over time after stimulation (*Fig. 2.8*). These data suggest that in response to group I mGluR stimulation mRNA granules/mRNPs can be delivered to excitatory synapses for a period following stimulation, and that this delivery requires FMRP.

Localization of GluR1 internalization.

Previous research has shown that dysregulated GluR1 internalization in *fmr1* KO neurons is associated with the lack of control of translation machinery [58]. To understand if internalization of GluR1 could be spatially localized, we further investigated the level of GluR1 internalization by staining of surface and internal GluR1 receptors at WT and KO dendrites and spines after group I mGluR stimulation. The ratio of internal staining versus total GluR1 staining was analyzed in WT and *fmr1* KO neurons, at 15 minutes after DHPG removal (*Fig. 2.9.a*). The level of GluR1 internalization was significantly elevated in WT spines after DHPG stimulation, but was not elevated in KO spines (*Fig. 2.9.b*). Furthermore, the stimulation-induced internalization in WT spines was blocked by the protein-synthesis inhibitor cycloheximide. In contrast, GluR1 internalization was elevated in the dendrites of non-stimulated KO neurons compared with WT dendrites, and stimulation with DHPG did not increase the level of dendritic internalization. KO

dendrites treated with cycloheximide alone also showed enhanced internalization compared with untreated WT dendrites, although dendrites treated with cycloheximide and DHPG together did not (*Fig. 2.9.c*). We also compared the enrichment of internalized GluR1 in spines with the adjacent dendritic area (*Fig. 2.9.d*). WT stimulated by DHPG showed a non-significant trend towards more internalization than did KO under the same conditions. Together, these data suggest that GluR1 internalization could fail to be localized in *fmr1* KO neurons as well as failing to respond to stimulation.

Discussion

We have presented evidence that FMRP can target mRNAs toward specialized locations for de novo protein synthesis and subsequent translation-dependent plasticity events. First, using time-lapse imaging, we showed that *Fmr1* and CaMKIIα RNA particles decelerated their motion during 0-40 minutes after group I mGluR stimulation and returned to their basal level of movement during a later stage. We hypothesized that during this early time period RNAs associated with FMRP might be targeted to specialized microenvironments for protein synthesis necessary for subsequent GluR1 internalization and other plasticity-related changes. Second, we showed that translation of FMRP occurs locally adjacent to mGluR5 rich regions. Third, our experiments using YFP-labeled spines revealed that endogenous CaMKIIα mRNAs and protein synthesis of CaMKIIα are enriched at spines compared with neighboring dendritic regions only in the presence of FMRP. Lastly, the internalization of GluR1 occurs at spines in WT neurons, but in dendrites of KO neurons after stimulation. Furthermore, internalization in KO dendrites appears to be constitutively higher in *fmr1* KO dendrites compared with WT dendrites. These data strongly corroborate our hypothesis whereby FMRP enhances RNA targeting to specialized regions for local translation in response to neuronal stimulation.

Using time lapse imaging, we observed that during the period 0-40 minutes after neurotransmitter treatment, mRNA granules exhibited slower motion than before stimulation. We speculated that this stage may represent the docking of mRNA granules based on evidence from the literature. First, it has been shown that the “hotspots” of

dendritic translation are spatially stable after stimulation and co-localized with ribosomes [31, 32]. Second, the selective association of FMRP between microtubules or polyribosome may provide translation initiation control [62]. Third, it has been demonstrated that FMRP-mRNP complexes relocate into dendritic spines after stimulation [48]. Lastly, Myosin Vα associates with another RNA binding protein, TLS, to localize mRNA into dendritic spines [47, 96, 97]. We have now shown quantitative data comparing the temporal and spatial distribution of CaMKIIα mRNA, CaMKIIα protein and GluR1 internalization in WT and *fmr1* KO neurons upon group I mGluR stimulation. Our data suggest that while dendritic translation events are spatially static, spines could be the targets for mRNA docking and protein synthesis in response to neuronal stimulation.

FMRP can also facilitate directional *Fmr1* mRNA granules/mRNPs movement (*Fig. 2.3.c*) at 40-60 minutes after group I mGluR stimulation. This agrees with a previous finding that in *dfmr* mutant neurons *CG9293* mRNA exhibits less directional movement [98]. The increased transport efficacy at 40-60 minutes suggests the heightened unidirectional movement in the presence of FMRP, which may be associating with motor proteins. mRNA granules/mRNPs could be carried by FMRP into the dendritic compartment from the soma; or mRNAs may be delivered toward nearby stress granules and/or P-bodies for storage or mRNA decay [99-102]. Alternatively, these translation-primed mRNAs may be transported to active synaptic regions and be deposited there for the next translation event to induce plasticity, including morphological and physiological changes in dendritic spines that may strengthen or weaken the synapse as necessary [103]. Further investigation will be required to elucidate the purpose and the mechanism of directional dendritic mRNA transport in response to neuronal stimulation.

In an earlier study, Dictenberg et al [65] compared CaMKIIα labeling granules movement in WT and *fmr1* KO dendrites. Under conditions of chronic (15 minutes) DHPG treatment, they found faster movement of granules in WT than KO. We also observed faster movement in WT dendrites under basal conditions. We then compared this basal movement to movement after acute (5 minutes) DHPG stimulation to imitate more closely a natural stimulation event. In this case, both CaMKIIα and *Fmr1* bearing

granules exhibited an initial decrease in movement, recovering to basal level after 40 minutes post-stimulation. In addition, we observed that the large motile particles become brighter after stimulation (*Fig. 2.3.d and 2.7.d*); we attribute this to aggregation with smaller sub-threshold particles. This would be in agreement with studies of mRNA transport dynamics, based on FRAP (fluorescence recovery after photobleaching) [63, 104], that showed rapid recovery of average fluorescence intensity in photo-bleached dendritic segment after stimulation.

FMRP mediated translation-dependent synaptic plasticity may be regulated at several levels. First, dendritic transport and synaptic docking of mRNA could regulate the availability of specific mRNAs for local protein synthesis. FMRP could regulate dendritic transport of specific mRNAs after neuronal stimulation [63, 65]. We have shown that FMRP can facilitate the localization of CaMKIIα mRNA (one of several mRNAs associated with FMRP) at dendritic spines for subsequent translation, lending support to the role of FMRP in regulatory synaptic delivery of specific mRNA. Second, the restriction of protein distribution by proteasome degradation could be important for synaptic function as well. mGluR-LTD induces a transient, translation-dependent increase in FMRP that is rapidly degraded by the ubiquitin-proteasome pathway [55]. Lastly, the involvement of miRNAs associated with FMRP in synaptic protein expression is also emerging [105, 106]. FMRP is critically involved in several levels of regulation of protein synthesis for synaptic plasticity and the current work suggests a dynamic role of FMRP in transport, spine localization, rapid translational control, and receptor internalization.

Figures

Figure 2.1 MS2 labeling strategy and its controls.

(a) Dual constructs for GFP labeling of mRNA were shown in Rook MS et al, 2000. Briefly, CaMKIIα 3'UTR was linked with eight copies of MS2 binding site RNA (MS2bs-CaMKIIα), which has strong affinity to MS2 protein. *Fmr1* ORF-3'UTR was subcloned to replace CaMKIIα (MS2bs-*fmr1*) to label *fmr1* mRNA. MS2 binding site RNA alone (MS2bs) was used as a negative control. GFP tagged MS2 with nuclear localization signal (GFP-MS2-nls) labeled CaMKIIα or *fmr1* mRNA via MS2-MS2bs interaction in live neurons.

a.

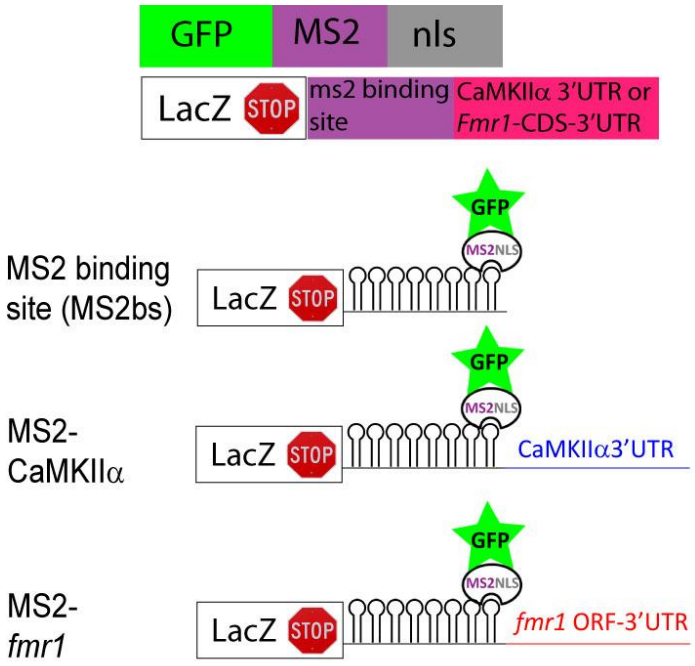

Figure 2.1 MS2 labeling strategy and its controls. (cont.)

(b) WT or *fmr1* KO neurons were transfected with GFP-MS2-nls and MS2bs-*fmr1*. GFP labeled *fmr1* form puncta (green) in dendrite. FMRP (red) appeared only in WT neurons by immunostaining, demonstrating that FMRP cannot be translated from MS2bs-*fmr1* construct. Scale bar, 10μm.

b.

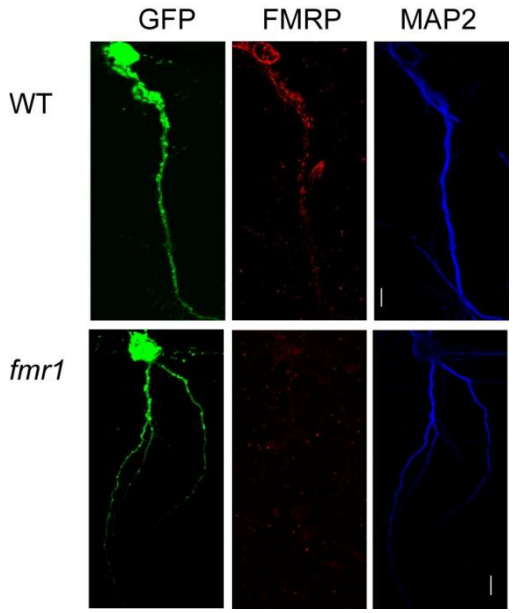

Figure 2.1 MS2 labeling strategy and its controls. (cont.)

(c) There is similar FMRP (red) distribution in mock-transfected or dual *fmr1*-labeling constructs transfected WT neurons; therefore nuclear localization signal (nls) on GFP-MS2-nls does not trap FMRP in the nucleus.

c.

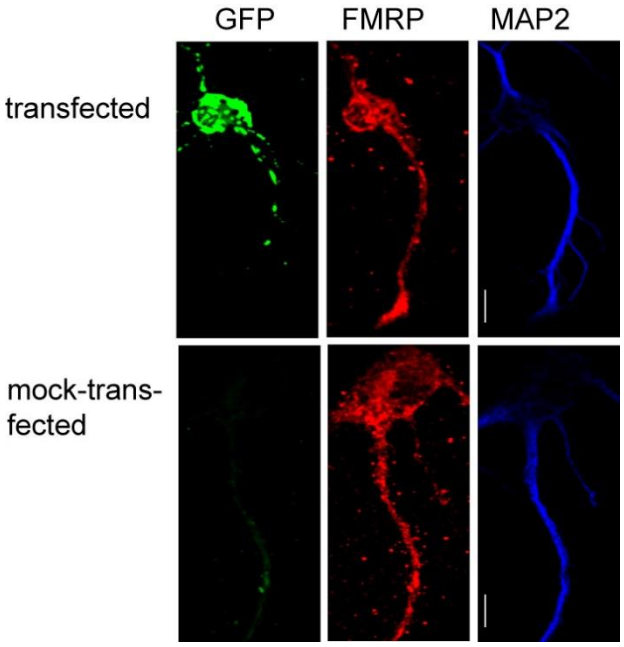

Figure 2.2 Labeling of CaMKIIα and *Fmr1* mRNA in primary hippocampal neurons.

(a) A neuron transfected with GFP-MS2-nls and MS2bs showed that GFP signals stay in soma. (b,c) The neuron transfected with GFP-MS2-nls and MS2bs-CaMKIIα or MS2bs-*fmr1* showed that mRNA puncta distribute in dendrites. Higher magnification of the boxed image showed GFP-labeled granules in dendrites.

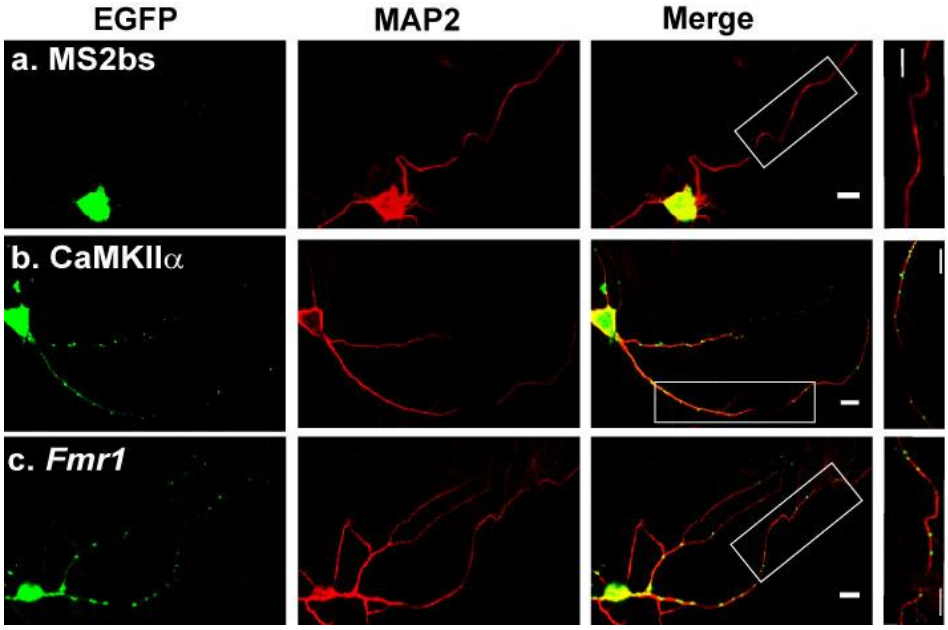

Figure 2.2 Labeling of CaMKIIα and *Fmr1* mRNA in primary hippocampal neurons. (cont.)

(d) *Fmr1* containing GFP-labeled granules (green) in dendrites colocalized with *Fmr1* mRNA detected by fluorescence in situ hybridization (FISH, red). Scale bar, 10μm.

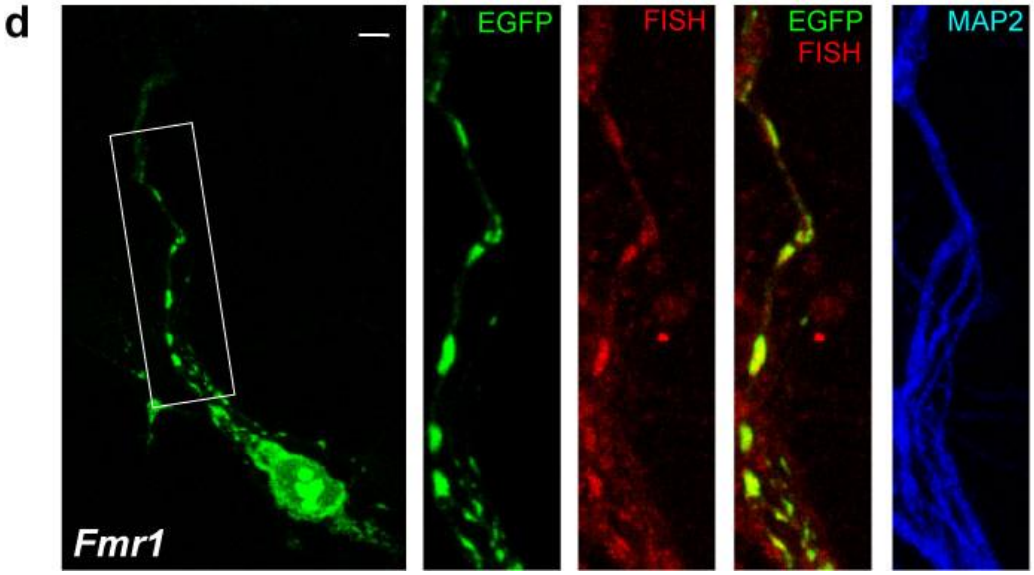

Figure 2.3 CaMKIIα and *Fmr1* mRNA dynamic motions in WT and *fmr1* KO hippocampal neurons.

(a) Representation of *Fmr1* mRNA movement in WT and *fmr1* KO neurons by time lapse imaging. Kymograph (upper) shows granule motion in the boxed region of a WT or KO neuron transfected with GFP-MS2-nls and MS2bs-*Fmr1*. The time point of image taken is labeled next to each kymograph, which represents a two-minute series of images at five-second intervals (25 frames in total). Scale bar, 20μm. Track length (lower) of each quantified *Fmr1* granule (arrowhead in kymograph) was represented. Track Length is the total length of displacements within the track.

a.

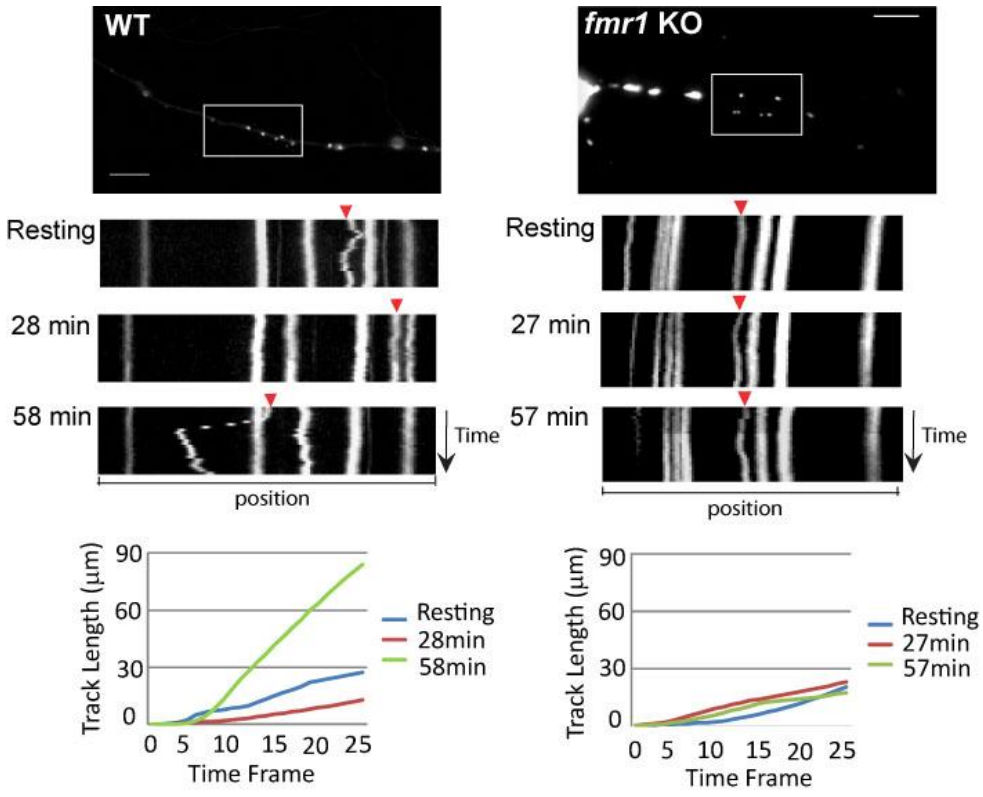

Figure 2.3 CaMKIIα and *Fmr1* mRNA dynamic motions in WT and *fmr1* KO hippocampal neurons. (cont.)

(b) Average speed of GFP labeled *Fmr1* or CaMKIIα mRNA calculated for WT or *fmr1* KO neurons, shows that particle movement was retarded in WT from 0-40 min after stimulation. (c) Directionality of GFP labeled *Fmr1* or CaMKIIα in WT or *fmr1* KO neurons was calculated, showing increased unidirectional movement of *Fmr1* mRNA in WT neurons. Bar graph represents data from 3 experiments, total of at least 20 mRNA particles in each group. Experiments and definition of average speed and transport efficacy were as described in methods. Statistical analysis by two-way ANOVA with Tukey HSD post test. Error bars denote SEM.

b.

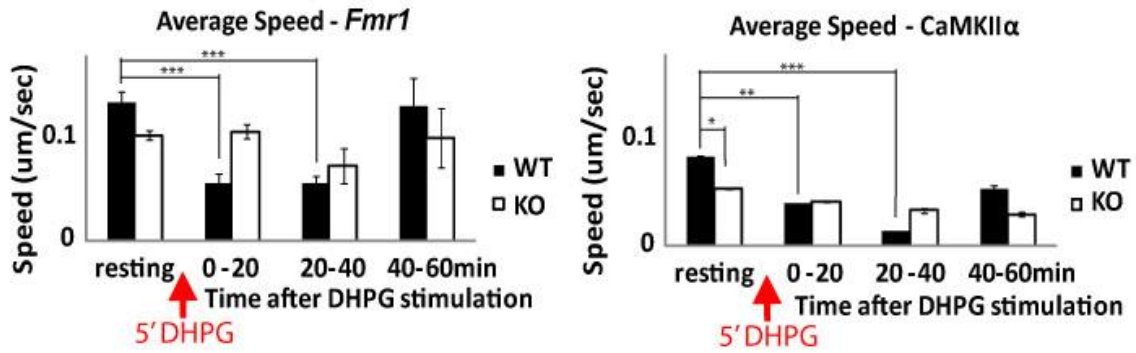

c.

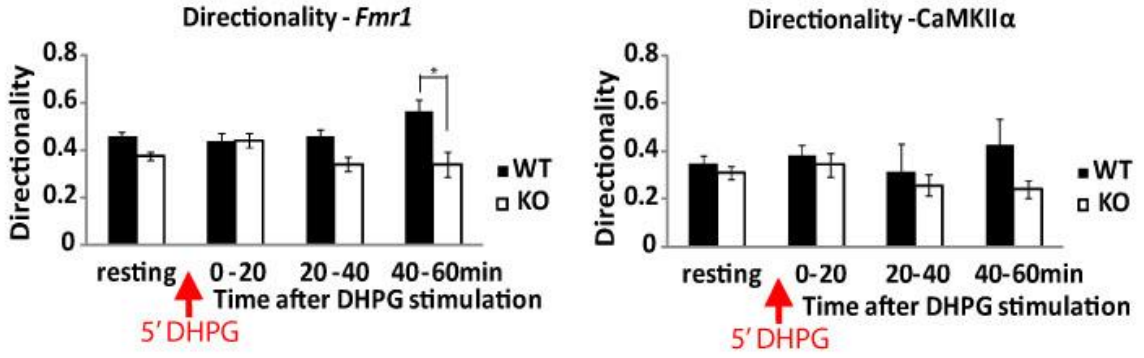

Figure 2.3 CaMKIIα and *Fmr1* mRNA dynamic motions in WT and *fmr1* KO hippocampal neurons. (cont.)

(d) The intensity of GFP labeled *Fmr1* mRNA in time lapse imaging was measured before or after DHPG treatment. The pair-wise comparison of granule intensity was only applied to the time series with exact imaging parameters before and after stimulation. Statistical analysis by two-tailed t-test. Error Bars denote SEM.

d.

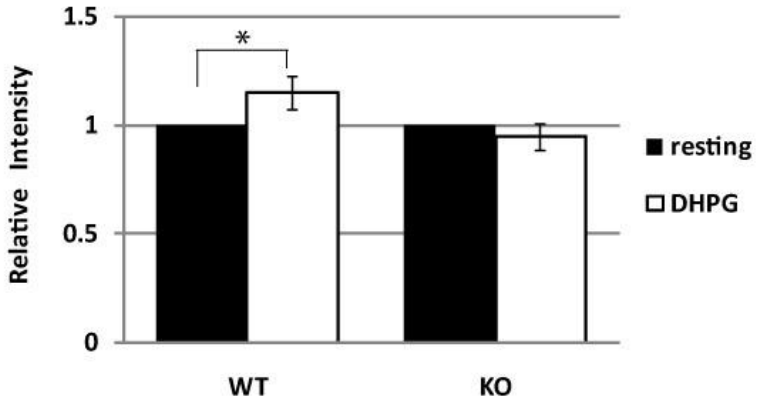

Figure 2.4 Colocalization between surface group I mGluRs and FMRP after DHPG treatment.

(a) Representative deconvolved image (Z projection) detected surface mGluR5 (red) and endogenous FMRP (green). Higher magnification of the boxed image shows that more FMRP colocalized with surface mGluR5 at 20 minutes after DHPG (yellow arrow), but not in the presence of CHX (cycloheximide). Scale bar, 20μm.

a.

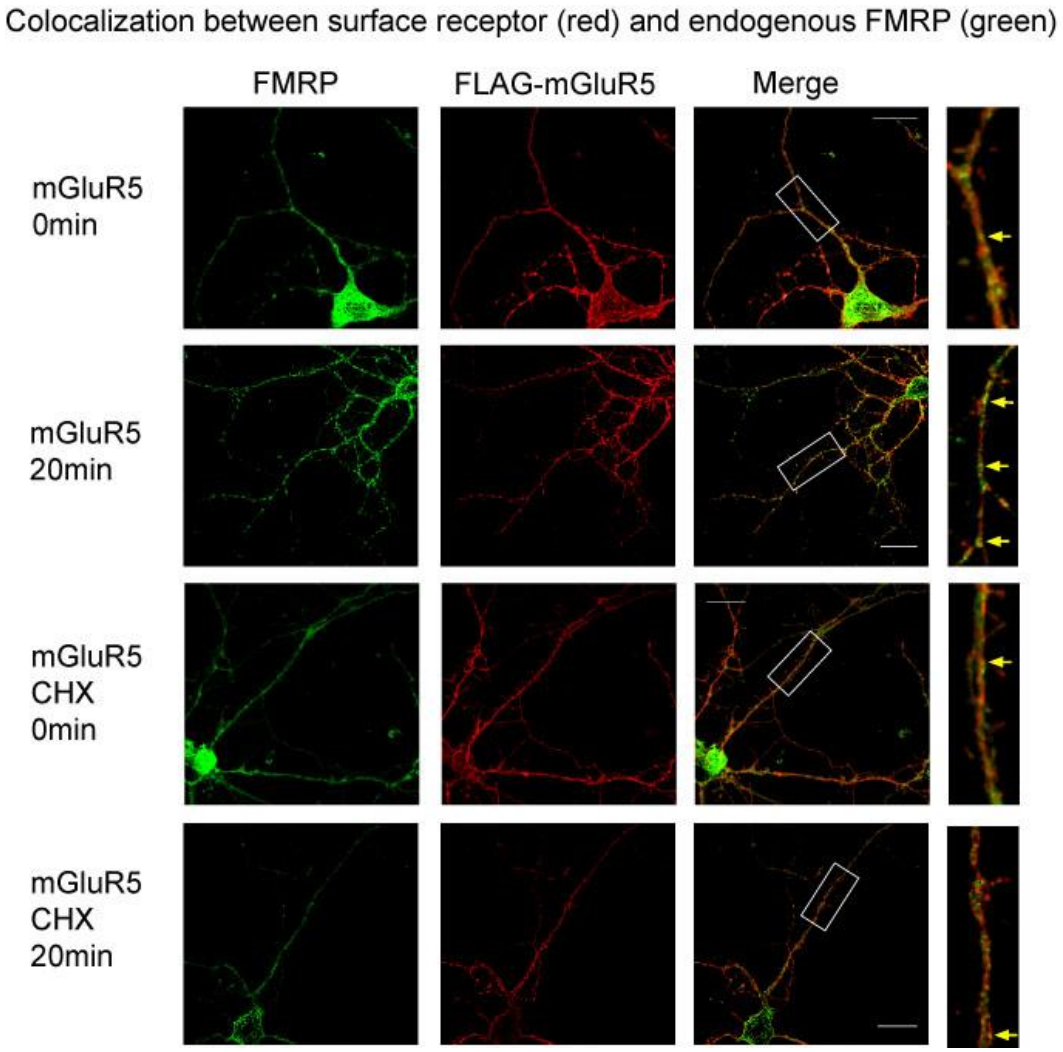

Figure 2.4 Colocalization between surface group I mGluRs and FMRP after DHPG treatment. (cont.)

(b-e) The increased colocalization between FMRP and surface mGluR5 at 20 min was measured as Mander's coefficient. The time points indicate the time post washout after 5-min DHPG incubation. Data were analyzed from at least 15 dendrites in each group, 3 independent experiments. Statistical analysis by one-way ANOVA with Dunnett's post test. Error bars denote SEM.

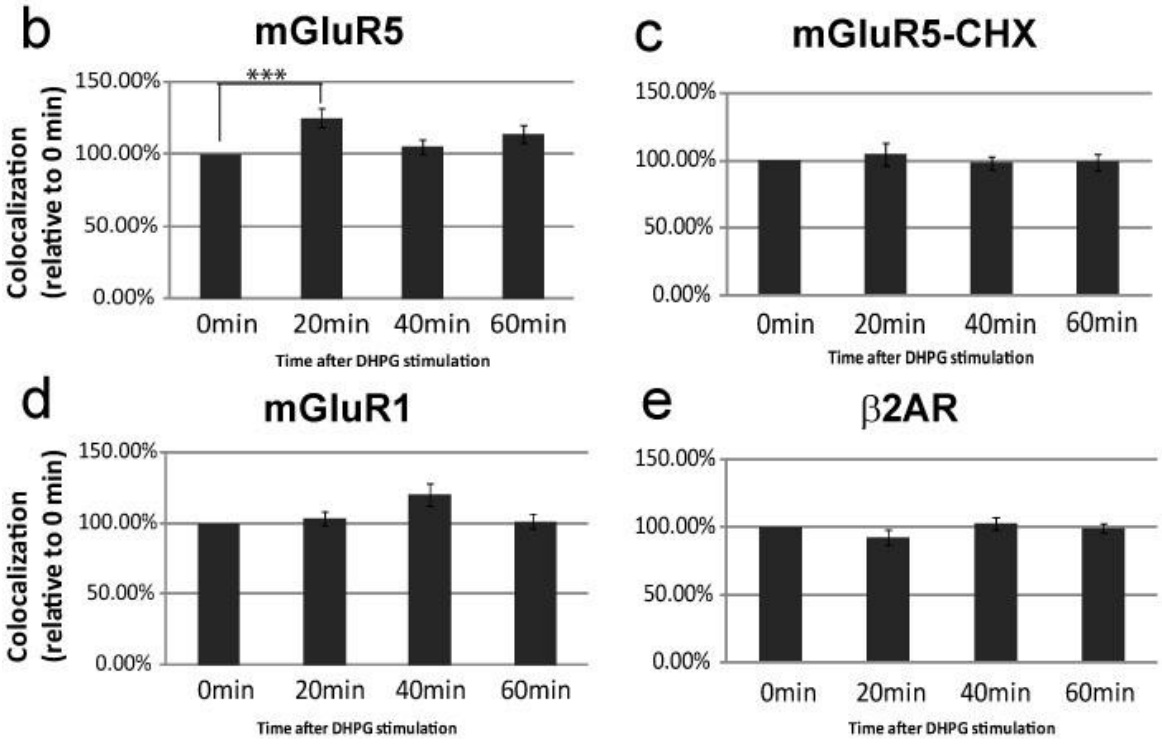

Figure 2.5 Controls for surface staining of FLAG tagged receptor and relative distribution of surface FLAG-receptor and endogenous receptors.

(a) Immunofluorescence (IF) of anti-FLAG (green) and anti-mGluR1a or anti-mGluR5 (red), which recognizes intracellular epitope of the receptor, was performed under non-permeant condition in FLAG-mGluR1a or FLAG-mGluR5 transfected hippocampal neurons. Only FLAG on cell surface can be stained but not the intracellular portion of endogenous mGluR1a or mGluR5. This shows that only the surface portion of receptors was labeled by this method.

a.

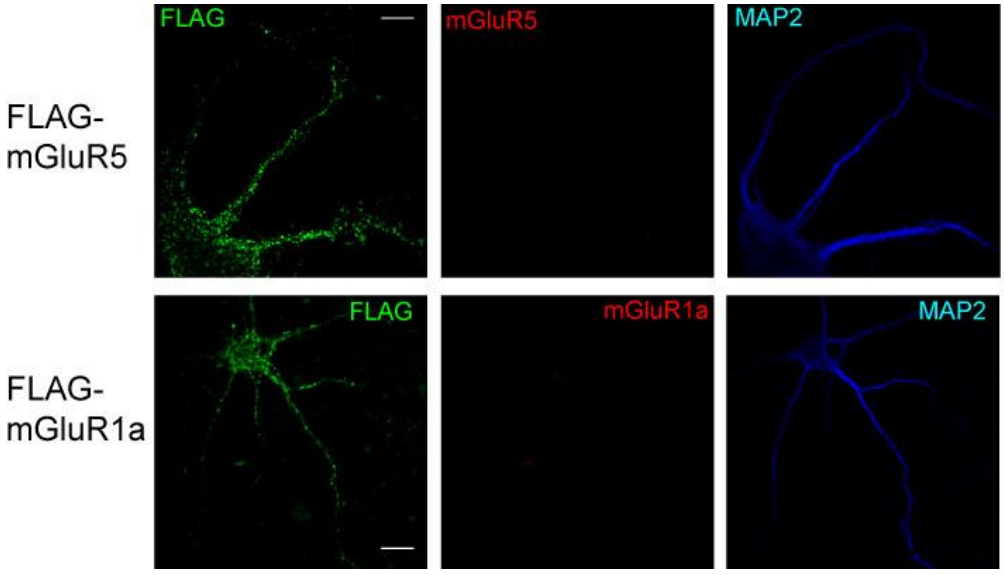

Figure 2.5 Controls for surface staining of FLAG tagged receptor and relative distribution of surface FLAG-receptor and endogenous receptors. (cont.)

(b) IF of surface group I mGluR was compared to the staining pattern of endogenous receptors. In *b1*, almost all surface staining of mGluR5 (green) corresponds with the staining of endogenous mGluR5 (red). However, in *b2*, the staining of surface mGluR1a (green) does not fully co-localize with endogenous mGluR1a (red). The relative distribution of surface mGluR5 versus endogenous mGluR1a (*b3*) and surface mGluR1a versus endogenous mGluR5 (*b4*), as negative controls, showed the degree of overlapping of two different receptors.

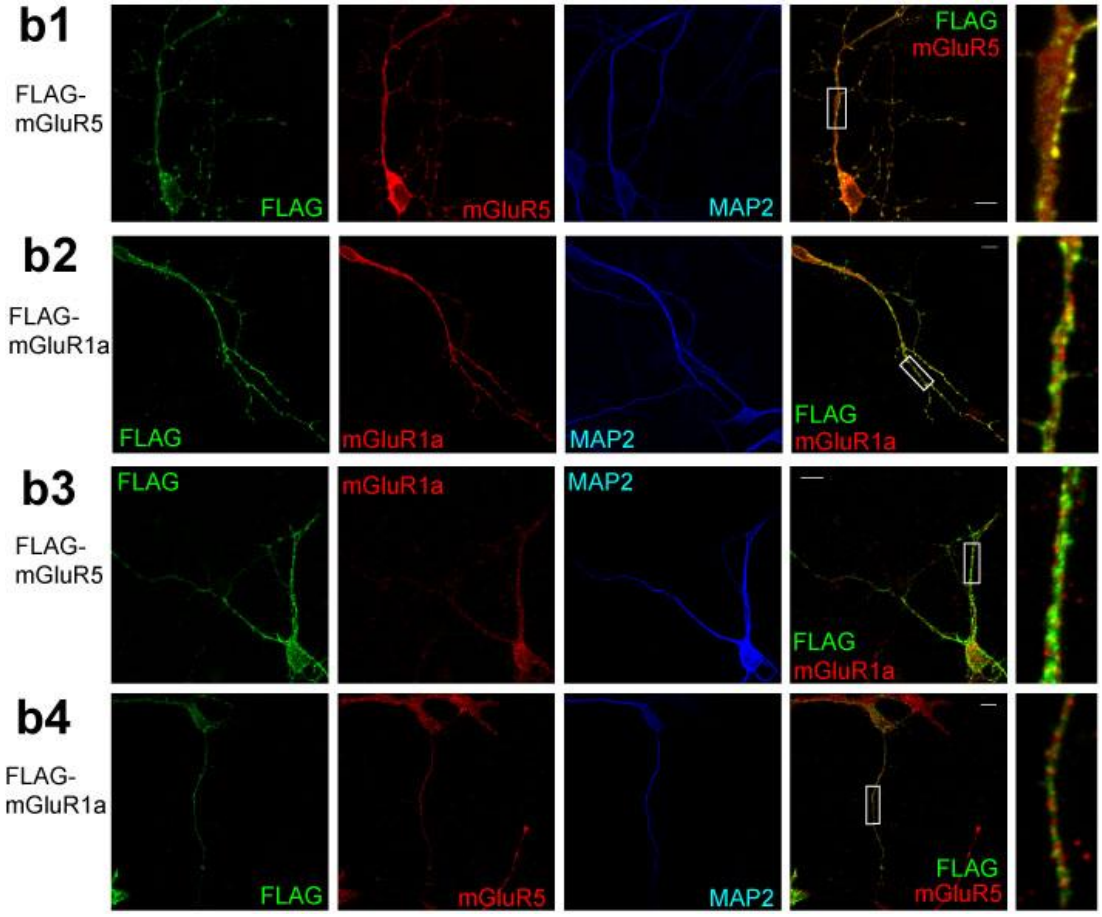

Figure 2.6 The differential distribution of CaMKIIα protein in neuronal spines and dendrites in response to group I mGluR stimulation. Cycloheximide blocks local translation of CaMKIIα in spines of WT neurons.

(a) Yellow fluorescence protein (YFP) expressing hippocampal neurons (green) were used to outline neuronal dendrites and spines. A higher magnification of the boxed region shows that spine (yellow) and neighboring dendrite (white) regions could be selected based on YFP staining threshold. Scale bar, 10μm. (b) Representative figures of CaMKIIα immunostaining (red) in WT or *fmr1* KO YFP hippocampal neurons showed relative CaMKIIα distribution in spines or dendrites in response to group I mGluR stimulation (DHPG).

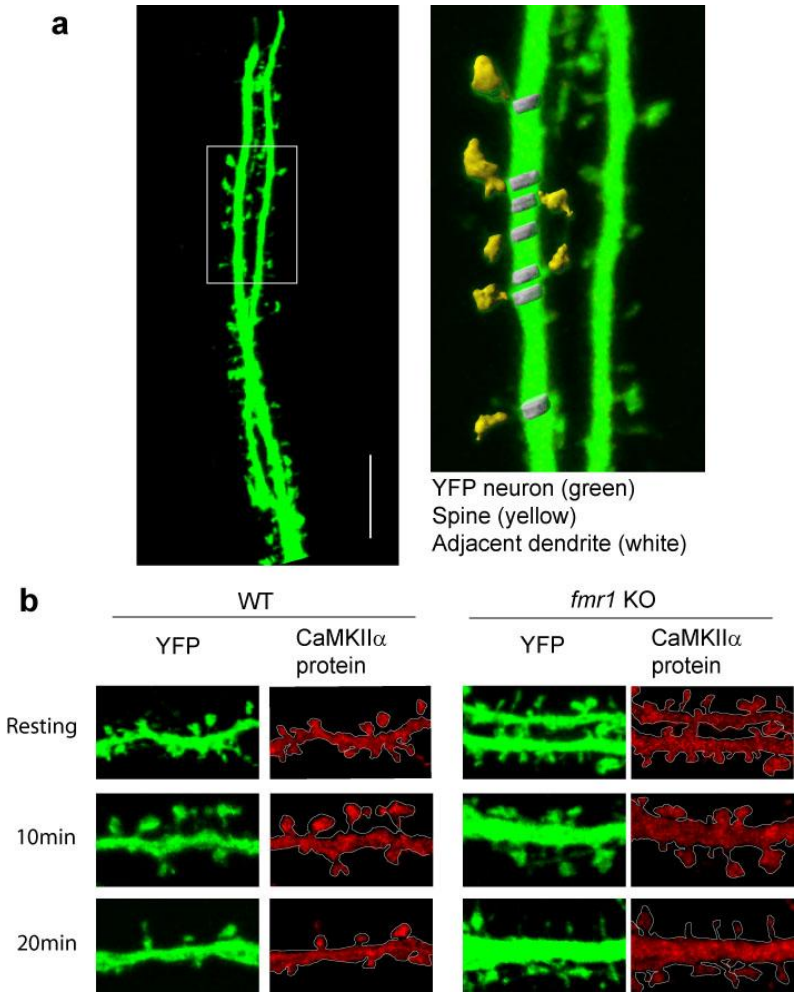

Figure 2.6 The differential distribution of CaMKIIα protein in neuronal spines and dendrites in response to group I mGluR stimulation. Cycloheximide blocks local translation of CaMKIIα in spines of WT neurons. (cont.)

(c, d) The average intensity of CaMKIIα protein in WT or *fmr1* KO YFP spines (c) or adjacent dendrites (d) was measured and compared to CaMKIIα level before stimulation. (e) Enrichment of CaMKIIα mRNA in spine relative to adjacent dendrite was calculated and normalized to the level before DHPG treatment. (f, g) In the presence or absence of 60μM cycloheximide, a protein synthesis blocker, throughout the experiment, the level of CaMKIIα in spines (f) or neighboring dendrites (g) of WT neurons was measured. (h) In the presence or absence of 60μM cycloheximide, the level of CaMKIIα in WT spines versus dendrites was calculated as the level of CaMKIIα in one spine divided by the level in the neighboring dendrite. Data were analyzed from at least 18 dendrites in each group, three independent experiments. Statistical analysis by two-way ANOVA with Tukey-HSD post test. Error bars denote SEM.

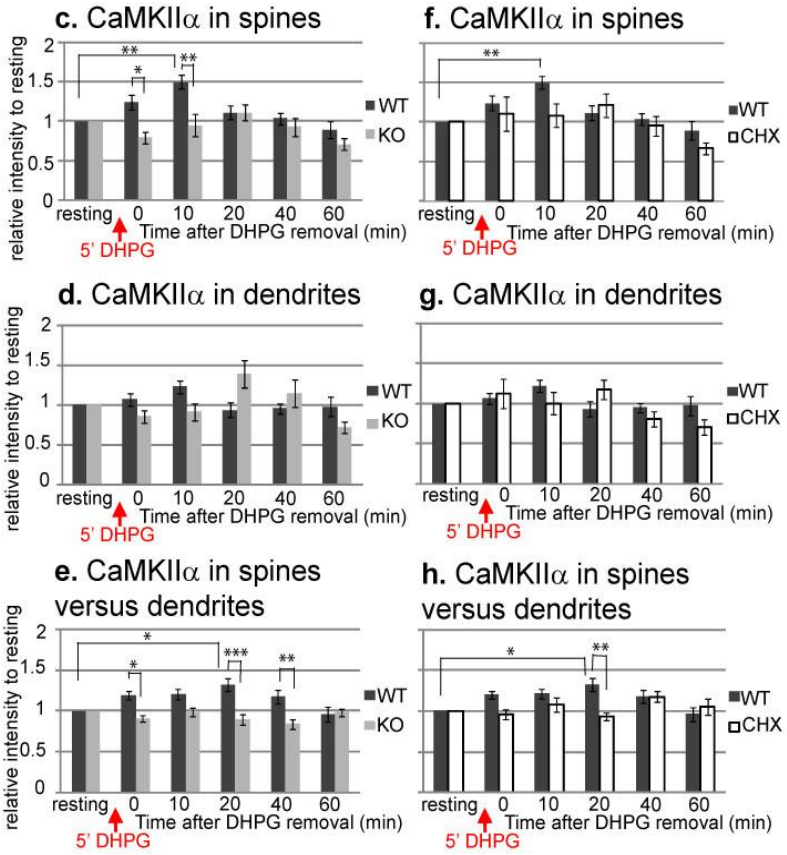

Figure 2.7 The differential distribution of endogenous CaMKIIα mRNA in neuronal spines and dendrites of WT or *fmr1* KO neurons in response to group I mGluR stimulation.

(a) FISH detected CaMKIIα mRNA (red) in dendrite of YFP hippocampal neurons (*left*). Hybridization with a sense probe showed no detectable labeling in dendrite (*right*). Scale bar, 10μm. (b) Two magnified figures of spines (arrows in A) showed that CaMKIIα mRNA could be localized in spine head, adjacent dendrite region (left), or spine base (right).

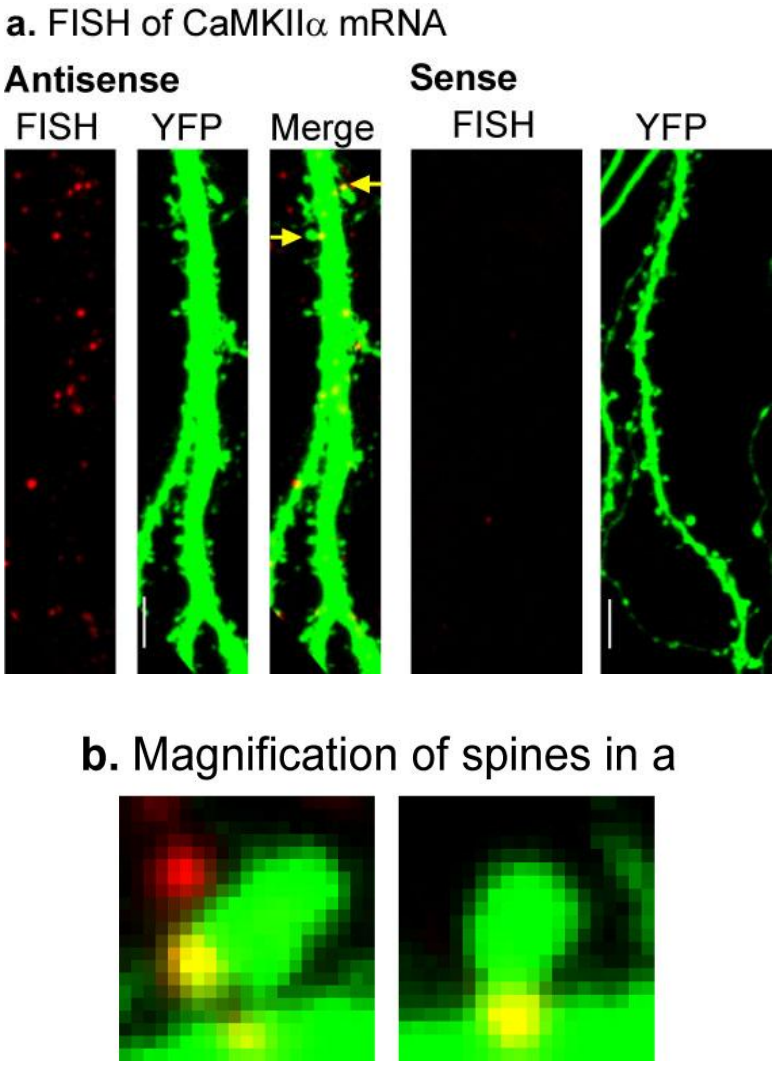

Figure 2.7 The differential distribution of endogenous CaMKIIα mRNA in neuronal spines and dendrites of WT or *fmr1* KO neurons in response to group I mGluR stimulation. (cont.)

(c) The number of CaMKIIα mRNA particles in 50μm dendrite segments was calculated in WT and *fmr1* KO neurons before or at different time points after 5 min DHPG treatment. (d) The average intensity of CaMKIIα mRNA was measured in each 50μm dendrite segment. The level of average intensity was compared to the level before DHPG stimulation in WT or *fmr1* KO neurons.

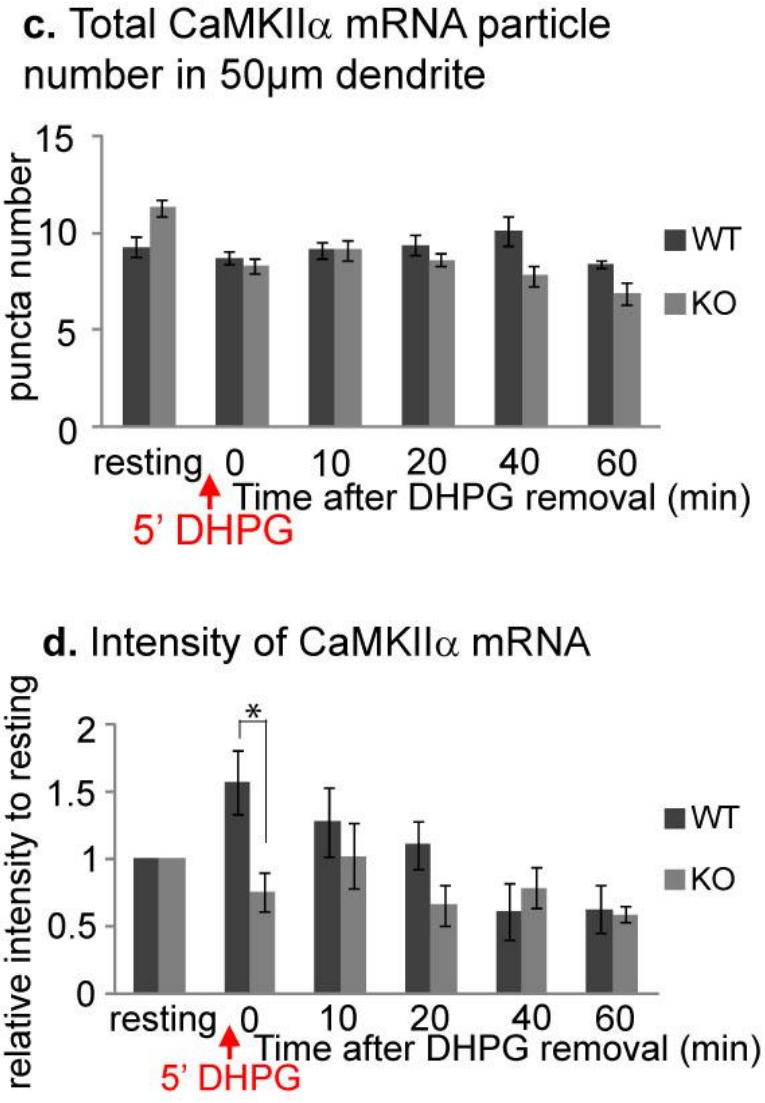

Figure 2.7 The differential distribution of endogenous CaMKIIα mRNA in neuronal spines and dendrites of WT or *fmr1* KO neurons in response to group I mGluR stimulation. (cont.)

(e) The ratio of the number of CaMKIIα mRNA localized in spines versus total number of CaMKIIα in each 50μm dendrite segment was calculated, showing a peak ratio immediately after DHPG stimulation in WT but not KO. Data were analyzed from at least 20 dendrites in each group, three independent experiments. In *c and d*, data were analyzed by two-way ANOVA with Tukey-HSD post-test. In e, the value of ratio was transformed to meet normality requirement and then analyzed by two-way ANOVA with Tukey-HSD. Error bars denote SEM.

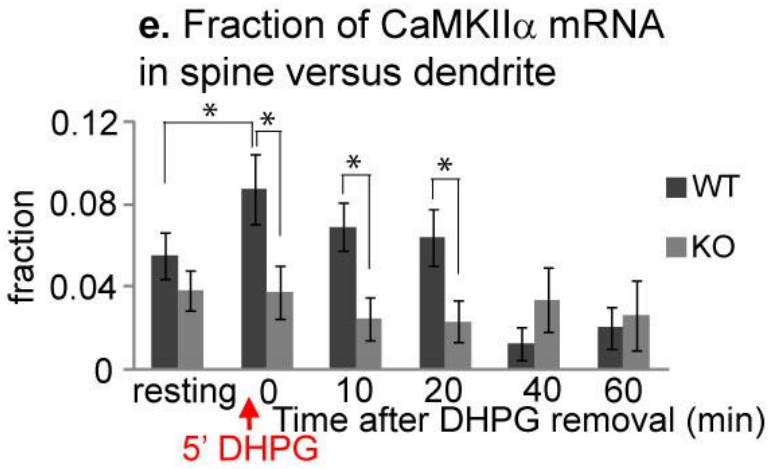

Figure 2.8 The distribution of polyA mRNA in neuronal dendrites or spines.

(a) Representative figures showing fluorescence in situ hybridization of polyA mRNA in YFP neurons (*upper*). The negative control, a probe to recognize polyT, did not show clear staining in neuronal dendrites (*lower*). (b, c) The intensity of polyA FISH was measured in spines (b) or adjacent dendrites (c) of YFP neurons. Statistical analysis by two-way ANOVA. Error Bars denote SEM.

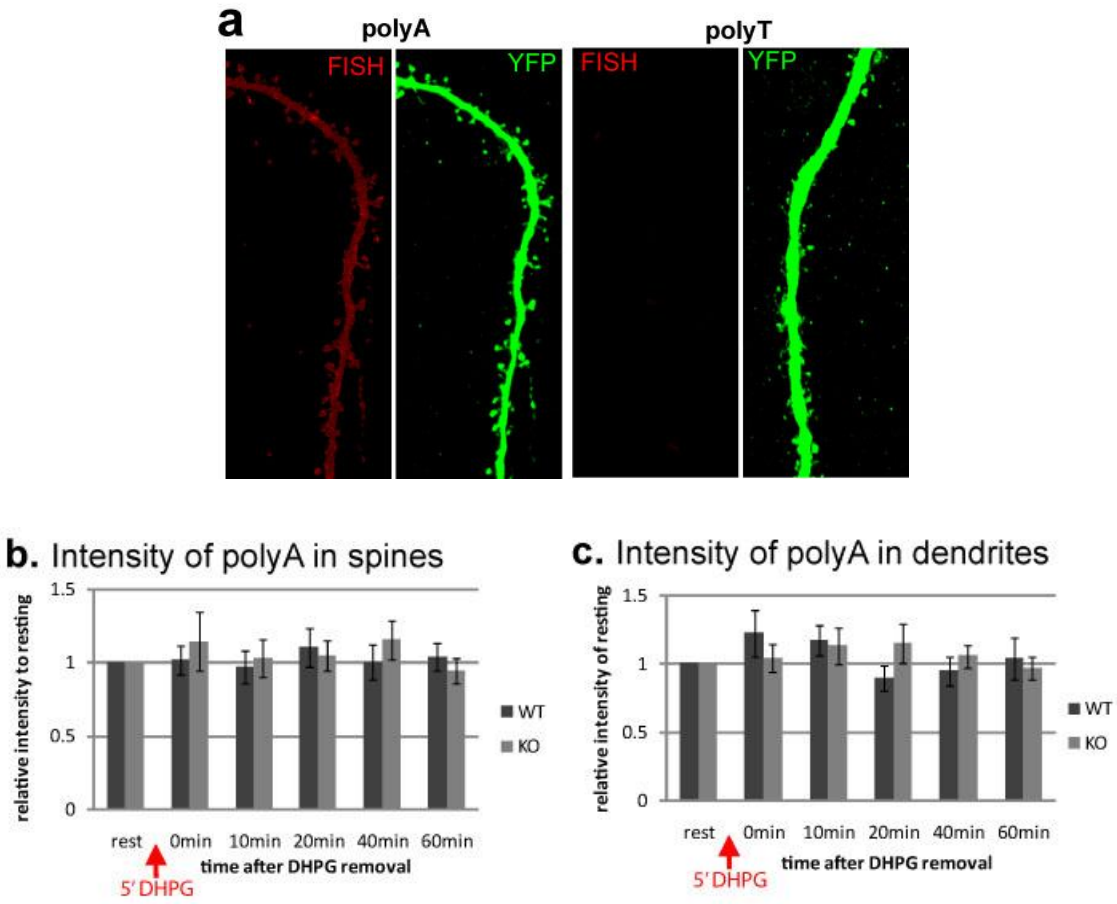

Figure 2.9 The level of GluR1 internalization in neuronal spines or dendrites 15 minutes after Group I mGluR stimulation.

(a) Representative images showing surface or internalized GluR1 in control or DHPG treated WT or *fmr1* KO neurons. Scale bar, 2μm.

a.

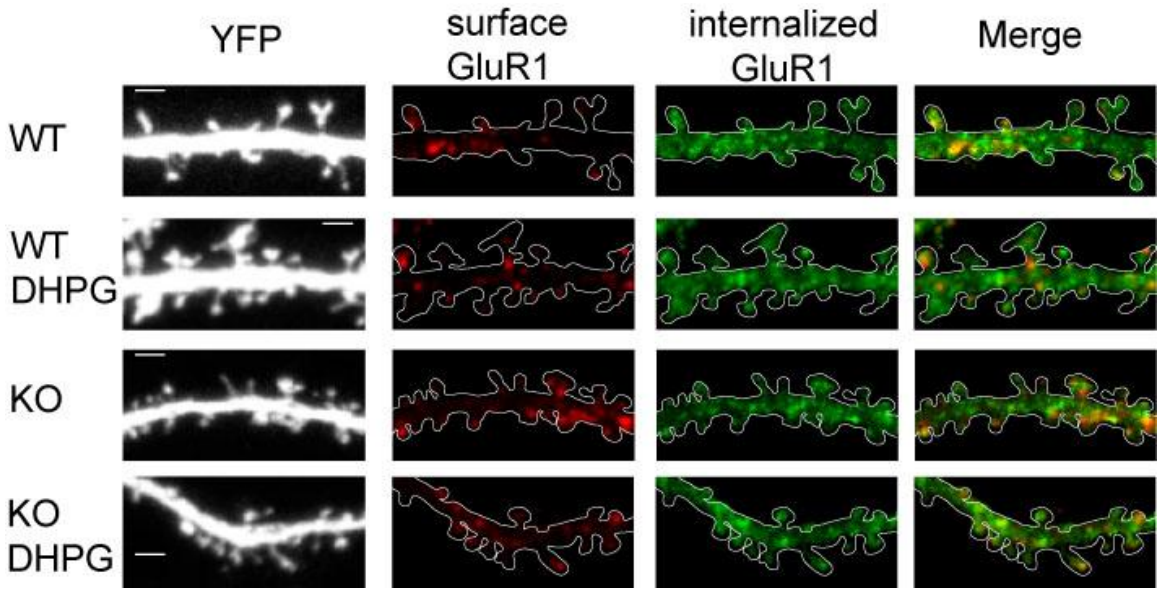

Figure 2.9 The level of GluR1 internalization in neuronal spines or dendrites 15 minutes after Group I mGluR stimulation. (cont.)

(b, c) The level of GluR1 internalization was measured in spine or dendrite regions defined by YFP. The internalization levels were compared to the level in WT control group. While WT neurons showed more spine internalization, *fmr1* KO neurons exhibited more dendritic internalization. (d) The level of GluR1 internalization per spine was compared to the level in the neighboring dendrite. Data were analyzed from at least 15 dendrites in each group, three independent experiments. Statistical analysis by two-way ANOVA and Dunnett's post test. Error Bars represent SEM.

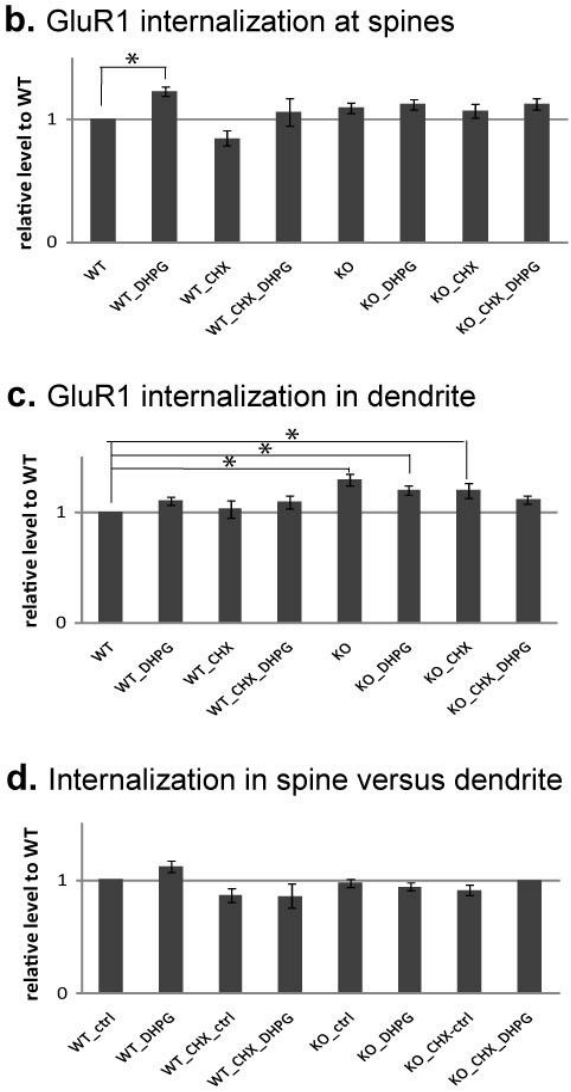

Chapter 3.

The role of FMRP isoforms in synaptic mRNA docking

Abstract

To better understand the function of individual FMRP isoforms and the potential for gene therapy in Fragile X Syndrome, we investigated their reactivity in synaptic mRNA targeting. We studied specific FMRP isoforms (iso1, iso2, iso7 and iso8) that differ with regard to the hydrophobic loop extended from KH2 domain and by serine 499 phosphorylation modification. By using time-lapse imaging, we found that EGFP labeled iso1 and iso7 granules can significantly decelerate following 5 minutes DHPG treatment in wild type neurons but not in *fmr1* KO neurons. However, reinstating iso1, iso7 or iso2 cannot restore CaMKIIα mRNA targeting to *fmr1* KO spines after DHPG treatment as observed in wild type spines. The data suggest that a single FMRP isoform was not sufficient to restore the function of synaptic mRNA delivery, but requires the presence of multiple isoforms.

Introduction

Fragile X syndrome (FXS) is the most common form of inherited mental retardation and is caused by the loss of function of the *FMR1* gene, which encodes fragile X mental retardation protein (FMRP) [1]. FXS affects 1 in 4000 males and 1 in 6000 females on average and is characterized by hyperactivity, attention deficits, autistic-like behaviors, and seizures [2]. Dendritic spine morphology in the cerebral cortex of FXS patients and in the *fmr1* KO mouse model shows more immature long thin spines than mature stubby, mushroom-shaped spines [8]. Furthermore, group I-mGluR dependent long term depression (LTD) in the hippocampus is exaggerated in the *fmr1* KO model [10]. These findings suggest that FMRP functions in synaptic development and plasticity.

Alternative splicing variants of FMRP are synthesized in response to group I mGluR stimulation [12] and environmental stimuli [107]. However, there are limited studies that differentiate diverse properties of FMRP splicing variants [84-86]. To better optimize the possibility of gene therapy in FXS [108], we investigated the function of individual FMRP splicing isoforms. The *FMR1* gene contains 17 exons and 4 possible alternative splicing sites [80, 82]. Alternative splicing affects the presence of exon12 and exon14, and the selective usage of splicing acceptors on exon15 and exon17 (Fig. 3.1.a). Because an intact KH2 domain and phosphorylation modification of serine 499 of FMRP are critical to maintain synapse number and modulate the translation process [41, 109], we are particularly interested in contributions to synaptic function that may be encoded by exon12 and exon15, which correspond to a hydrophobic extension loop of KH2 domain and a fragment containing serine 499, respectively. Interestingly, the absence of exon12 can enhance the association between FMRP and an RNA segment called the "kissing complex" [84, 110], even though there is not as yet an identified FMRP-associated mRNA containing the kissing complex. Therefore, we characterized the properties of dynamic motions and synaptic targeting of CaMKIIα mRNA of FMRP iso1, iso2, iso7 and iso8, displaying differential splicing of exon12 and/or the phosphorylation site in exon15 (Fig. 3.1.b).

Fmr1 exon12 and exon15 mRNA splicing variants showed disparate RNA abundance. Approximately 80% of *Fmr1* mRNA in mouse brain lack exon12 due to alternative splicing [80]. Throughout development, *Fmr1* lacking exon12 is more abundant in brain tissues. However, in mouse cortex synaptosomes, *Fmr1* containing exon12 is more enriched than those lacking exon12 [84], suggesting that *Fmr1* containing exon12 could be enriched in synapses. Among three splicing acceptors (a, b and c) on exon15, exon15a is used most frequently in both adult and embryonic brain tissue [84]. So far, it is still technically problematic to distinguish FMRP isoforms at protein level, including using 2D-gel [111]. Therefore, the relative content of each FMRP isoform is still unclear.

In this study, we investigated dynamic movement of single FMRP isoforms, and isoform regulation of synaptic docking of CaMKIIα mRNA in neuronal dendrites. To better understand the regulatory role of a KH2 extension loop (exon12) and serine499

phosphorylation (exon15), we characterized iso1, iso2, iso7 and iso8, on which exon12 and exon15 are alternatively spliced.

Materials and Methods

DNA constructs.

EGFP-*Fmr1* isoform plasmid was generated by inserting *Fmr1* isoform cDNA into a pEGFP-C1 (Clontech) vector using EcoRI and XhoI. pIRES-EGFP-mRFP-*Fmr1* isoform was constructed by sequential insertion of the *Fmr1* 3' UTR PCR fragment and mRFP-*Fmr1* isoform cDNA into pIRES-EGFP (Clontech) vector. All plasmids were sequenced to verify their composition.

Primary hippocampal neuron culture and transfection.

Primary neurons were prepared from hippocampi of WT or *fmr1* KO C57BL/6 mice at postnatal day 1 to 2 and maintained in Neurobasal medium supplemented with B27 and Glutamax (Invitrogen). Neurons were transfected using Lipofectamine LTX (Invitrogen) at postnatal day 7 and maintained to the age indicated in each experiment. All studies were performed in compliance with the Institutional Animal Care and Use Committee of University of Illinois at Urbana-Champaign.

Time lapse imaging.

Primary WT or *fmr1* KO hippocampal neurons were transfected and imaged within 24 hours post-transfection. Neurons were maintained in Liebovitz's L-15 (Invitrogen) supplemented with B27 (Invitrogen) at 37^{o}C in a 5% CO2 live-cell incubation chamber and imaged using the 40X objective (NA 1.4) on a Zeiss Axiovert 200M microscope, before and after exposure to 50μM (S)-3,5-Dihydroxyphenylglycine (DHPG, Tocris), an mGluR group I agonist, for 5 minutes. Images were taken every 5 seconds for 25 frames.

Imaging analysis.

For time-lapse imaging, granules consistently motile during at least two time points were analyzed. Time-lapse imaging series were analyzed by ImarisTrack software (Bitplane). Total trafficking length of motile particles was measured and divided by time as average

speed. The Track Displacement is the distance between the first and last position. The Track Length is the total length of displacements within the track. The track efficacy, calculated by track displacement divided by track length, is the measurement of unidirectional movement. Fluorescence recovery after photobleaching (FRAP) images were taken every 10 seconds for 5 minutes while three images were taken before photobleaching on a Zeiss 710 confocal microscopy. FRAP data were presented by percentage of recovery of the GFP intensity comparing to the intensity level before photobleaching as 100% and after photobleaching as 0%. The mobile fraction is determined by comparing the fluorescence intensity in the bleaching region after equilibrium is reached (I_∞) with the intensities before (I_i) and immediately after (I_0) bleaching. The mobile fraction (I) is defined as: $I= (I_\infty–I_0)/ (I_i-I_0)$ [112]. All imaging and bleaching parameters were kept the same during three replicates.

Fluorescence in situ hybridization.

Digoxigenin (DIG) labeled riboprobes were generated from plasmids with T3 or T7 RNA polymerase sites. Primary neurons were fixed with 4% paraformaldehyde, permeabilized with methanol, and then prehybridized with hybridization buffer. Then neurons were incubated with probes in hybridization buffer overnight at 55^{o}C for CaMKIIα probes, described previously [113]. After hybridization, cells were washed serially in 0.5X SSC with 50% formamide, 0.5X SSC and PBS. Neurons were incubated in primary antibody (chicken anti-GFP, AbCam) at 4^{o}C overnight and Cy2-anti-chicken (Jackson Immuno Research). Cells were then incubated with an HRP-linked DIG antibody (Roche) and the signal was amplified by Cy5 TSA-Plus system (PerkinElmer). Images were taken by Zeiss LSM710 with a 63X (NA1.4) objective as Z-stacks with a 0.3μm interval. All images in a single group were taken under the same acquisition parameters for relative comparisons.

Statistical analysis.

For mean comparisons, independent t-test, one-way or two-way ANOVA was performed. Tukey's HSD was carried out as post-hoc analysis as mentioned in figure legends. In all figures, data were presented as mean ± SEM, and *p<.05, **p<.01, ***p<.001.

Results

EGFP labeled iso1 and iso7 granules decelerated in wild type neurons following stimulation.

To investigate the dynamic motion of FMRP isoforms affected by either the hydrophobic loop extended from KH2 domain or the phosphorylation site (serine 499) on exon15, we examined the speed of EGFP tagged FMRP iso1, iso2, iso7 and iso8 following DHPG treatment (Fig. 3.2). To elucidate if a single FMRP isoform is sufficient we compare its dynamic motion when the single isoform was expressed in *fmr1* KO neurons (with no FMRP) with the motion in wild type neurons (with a full array of FMRP isoforms). Transfected neurons were imaged by time-lapse microscopy within 24 hours after transfection to keep exogenously expressed FMRP at a low level.

Iso1, the full length FMRP, exhibited retarded motion at 0-20 minutes after DHPG treatment in only wild type neurons (Fig. 3.2.a), as previously observed [113]. The speed of iso1 in wild type neurons was significantly reduced from 0.128±0.018μm/sec before stimulation to 0.061±0.006μm/sec at 0-20 minutes after DHPG removal ($p<0.05$, Tukey post test). In *fmr1* KO neurons, there was no retardation of movement. This result suggested that the change mobility of iso1 granules requires the presence of other isoforms.

Iso2, which contains a hydrophobic loop from the KH2 domain but not the phosphorylation site of serine 499, actually exhibited faster movement in the absence of other isoforms (0.180±0.034μm/sec in *fmr1* KO versus 0.091±0.016μm/sec in wild type neurons, $p<0.05$, Fig. 3.2.b), especially at 0-20 minutes after DHPG removal. This suggests that FMRP isoforms other than iso2 might act as a brake to decelerate RNA granules upon group I mGluR stimulation.

Iso7, which contains the phosphorylation site of serine 499 but not a hydrophobic loop from the KH2 domain, slowed down after stimulation but the deceleration is statistically significant only in wild type neurons (0.132±0.014μm/sec before stimulation comparing to 0.082±0.011μm/sec at 0-20 min ($p<0.05$), 0.074±0.006μm/sec at 20-40 min ($p<0.01$),

and 0.074±0.012μm/sec at 40-60 min ($p<0.01$) after DHPG removal, Fig. 3.2.c). The response to stimulation was similar to iso1; only in the presence of other isoforms was iso7 able to effectively decelerate.

Iso8, which contains neither a hydrophobic loop of the KH2 domain nor the phosphorylation site serine 499, did not significantly alter its speed over one hour time course after DHPG removal (Fig. 3.2.d) in both wild type and *fmr1* KO neurons. Although there was a trend towards slower motion at 20-40 minutes after DHPG removal, especially in wild type neurons, it is not statistically significant.

The data suggest that iso1 and iso7 may be the main contributors to mRNA granule deceleration in response to group I mGluR stimulation. More importantly, they cannot perform the function effectively without the presence of other isoforms.

Spine targeting of CaMKIIα mRNA in fmr1 KO could not be restored by introducing a single FMRP isoform.

We next investigated if a single FMRP isoform is able to localize CaMKIIα mRNA to *fmr1* KO spines as shown previously [113]. We designed constructs carrying mRFP alone or single mRFP tagged isoforms together with IRES-EGFP. By introducing the tandem construct at DIV7, spine morphology can be labeled by EGFP and mRFP-isoform will conduct its functions in the same neuron. At DIV19 to 21, neurons were stimulated by 50 μm DHPG for 5 minutes and endogenous CaMKIIα was labeled by fluorescence in situ hybridization. Total number of CaMKIIα puncta (> 0.3 μm) within every 50 μm dendritic segment did not change over one hour after group I mGluR stimulation (*Fig. 3.3*).

The fraction of CaMKIIα mRNA in spines of wild type neurons transfected with pIRES-EGFP-mRFP was highest at 0 minutes after stimulation and decreased for the following 60 minutes (0.059±0.013 before stimulation versus 0.148±0.027 at 0 minute after stimulation in WT neuron, $p<0.05$, *Fig 3.4.a*), but not in transfected *fmr1* KO neurons, consistent with our previous results [113].

In WT neurons transfected with pIRES-EGFP-mRFP-iso1 (*Fig. 3.4.b*), there was still a significant elevation of CaMKIIα mRNA fraction localized in spines at 0 minutes following DHPG removal, indicating the addition of iso1 did not alter the response (0.045±0.013 before stimulation versus 0.139±0.025 at 0 minutes after stimulation in WT neurons, $p<0.05$, *Fig. 3.4.b*). The fraction of CaMKIIα mRNA in iso1 transfected *fmr1* KO spines was only slightly increased at 10 min after DHPG treatment.

Interestingly, after introducing pIRES-EGFP-mRFP-iso7 into wild type neurons, we found that the fraction of CaMKIIα localized in spines peaked at 10 minutes after DHPG treatment (0.050±0.013 before stimulation versus 0.132±0.022 at 10 minutes after stimulation in WT neurons, $p<0.05$, *Fig. 3.4.c*) instead of 0 minutes in control group (*Fig. 3.4.a*). Again, introduction of iso7 did not restore CaMKIIα localization in *fmr1* KO spines either.

In WT neurons transfected with pIRES-EGFP-mRFP-iso2, there was an elevated fraction of CaMKIIα localized in spines at 0 minutes after DHPG removal (0.062±0.011 before stimulation versus 0.133±0.026 at 0 minutes after stimulation in WT neurons, $p<0.05$, *Fig. 3.4.d*). This may have been contributed by other endogenous FMRP isoforms since iso2 does not decelerate efficiently (*Fig. 3.2.b* in WT neurons). Iso2 did not restore CaMKIIα spine localization in *fmr1* KO. The data suggest that a single FMRP isoform, which we tested here, is not sufficient to completely restore the activity of synaptic mRNA delivery in *fmr1* KO neurons to the level of WT.

Discussion

In this study, we investigated the dynamic motions of four FMRP isoforms and determined their sufficiency to target CaMKIIα mRNA to spines following group I mGluR stimulation. We found that phosphorylation modification at serine 499 is critical to determine the behavior of FMRP-bearing granules before and after group I mGluR agonist stimulation. After stimulation, but only in the presence of other isoforms, iso1 and iso7 can decelerate efficiently; the speed of iso2 and iso8 did not alter significantly.

Although iso1 and iso7 displayed DHPG-induced deceleration of granules, nevertheless, when FMRP iso1 and iso7 were introduced to *fmr1* KO neurons, CaMKIIα mRNA was not localized to spines at the same level as in WT. These data suggest that the four specific isoforms tested here were singly not sufficient to restore FMRP activity in synaptic mRNA delivery in *fmr1* KO neurons.

We observed that in proximal dendrites there were also fast-moving small particles, but that are difficult to track across frames to measure speed, as reported previously [63, 98]. We therefore next used FRAP to measure the kinetics of these small EGFP labeled particles, caused by both active transport and diffusion. A higher score for percentage of recovery and mobile fraction results from higher motility of small particles moving from the non-bleached to the bleached area. The motility of small particles of iso2 and iso8 (*Fig. 3.5.b and d*), which do not contain the serine 499 phosphorylation site, elevated dramatically upon DHPG stimulation compared to iso1 and iso7 (*Fig. 3.5.a and c*). This might be because before stimulation iso1 and iso7 small particles exhibited greater motility than iso2 and iso8. More dynamic FMRP small particles in response to DHPG is also consistent with the previous report [63]. The data suggest that phosphorylation modification of FMRP is a critical determinant of its kinetics before and after group I mGluR stimulation.

Our data suggested that phosphorylation in serine 499 is critical to determine FMRP speed (*Fig. 3.2*) and kinetics (*Fig. 3.5*). When there is no serine 499 (iso2 and iso8), FMRP cannot decelerate in response to group I mGluR stimulation (*Fig. 3.2.b and d*). The phosphorylation of FMRP is regulated by S6K1 and PP2a [114, 115]. Previously, Ceman et al. [41] found that phosphorylation in serine 499 of FMRP could regulate FMRP in active or stalled translation elongation state, which could be mediated by miRNA pathway [105]. More importantly, phosphorylation of FMRP is also critical to regulate synapse number [109]. More studies need to be done to associate phosphorylation regulation of FMRP with mRNA docking and translation mechanism.

We also measured directionality of EGFP labeled isoforms as described previously [113]. We found that directionality of iso1, iso2 and iso7 reduced at 0-20 minutes upon DHPG

removal only in the presence of other isoforms (in WT neurons, *Fig. 3.6*). Kosik et al [29] have also suggested that one subset of granules oscillates near a cluster of synapses. We hypothesized that the slowed motion and enhanced oscillation in response to DHPG could result from FMRP targeting and docking to synapses.

The function of an individual FMRP isoform could be determined by the association with its interacting proteins. The motility of dendritic delivery of FMRP isoforms may be highly associated with interaction with motor proteins, such as KHC, KIF3C, DHC and myosinVα, and how that association is regulated by neuronal stimulation [60, 61, 65, 97]. The gene product of two autosomal homologues of the FMR1 gene, FXR1 and FXR2, can form oligomers with FMRP [116]. Although FXR1P is more highly expressed in muscle cells [117, 118], FXR2P has overlapping functions in neurons with FMRP [119, 120]. CYFIP1/2 (cytoplasmic FMRP interacting proteins) in *Drosophila* can interact with dFMR1 biochemically and genetically to regulate cytoskeleton remodeling downstream of Rho GTPase pathway [121, 122]. NUFIP1 (nuclear FMRP interacting protein) and 82-FIP, two other FMRP associated proteins, are involved in nucleocytoplasmic shuttling and cell cycle dependent localization of FMRP, respectively [123-125]. The association between any single FMRP isoform and other isoforms and its interacting proteins is implicated in individual isoform function.

The interaction between FMRP isoform and its associated mRNA and polyribosomes will also be an important question to answer. FMRP associated mRNAs, such as CaMKIIα [55], PSD-95 [56], and MAP1b [57], are highly involved in synaptic function. Whether there is specificity between FMRP isoform and mRNA targets could determine if single isoform or multiple isoforms will be required to restore function in *fmr1* KO neurons. From another perspective, FMRP association with polyribosome is mediated by mRNA [52]. The I304M mutation of FMRP disrupts its association with polyribosome [126], yet it has not been studied if the splicing of *Fmr1* exon12 affects FMRP association with polyribosomes. It is conceivable that the specificity between FMRP and mRNAs will alter FMRP association with polyribosomes.

Our data suggest that the serine 499 phosphorylation site is important to determine the speed of FMRP isoforms, which we examined here. More importantly, a single FMRP isoform is not sufficient to restore synaptic mRNA targeting function in *fmr1* KO *in vitro*. More molecular and biochemical properties of single isoforms will need to be determined in the future. The *fmr1* KO mouse could be used a model for assessing the roles of combined FMRP isoforms, with the eventual goal of patient therapy.

Figures

Figure 3.1 Alternative splicing of *Fmr1*.

(a) Alternative splicing affects the presence of exon12 and exon14, and the selective usage of splicing acceptors on exon15 and exon17.

(b) *Fmr1* iso1, iso2, iso7 and iso8, on which exon12 and exon15 with corresponding phosphorylation site are differentially spliced, were characterized here. FMRP iso1 is the full length protein; iso2 does not contain serine 499; iso7 does not have a hydrophobic loop extended from KH2; and iso8 does not contain either.

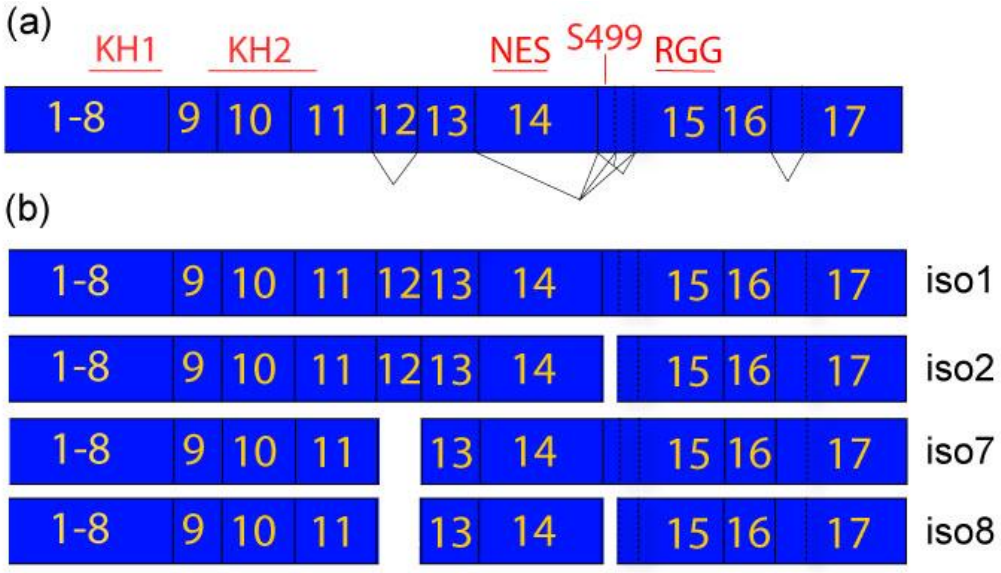

Figure 3.2 Speed of EGFP-FMRP isoforms

(a) In WT neurons, the speed of EGFP-labeled iso1 was significantly reduced at 0-20 minutes after DHPG stimulation. (b) In *fmr1* KO neurons, iso2 was significantly faster than in WT neurons at 0-20 minutes after DHPG. (c) In WT neurons, the speed of iso7 was significantly reduced after DHPG stimulation. (d) Iso8 does not alter speed significantly over one hour after DHPG removal. Bar graph represents data from at least three independent experiments, total of at least 40 mRNA particles in each group. Statistical analysis by two-way ANOVA with Tukey HSD post test. Error bars denote SEM.

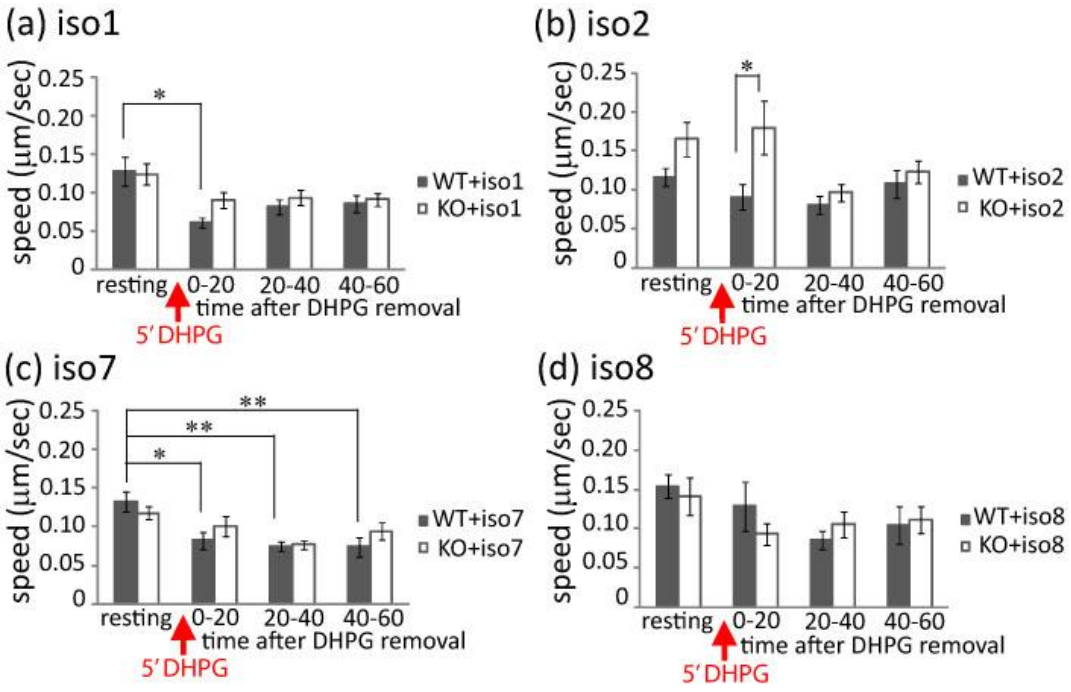

Figure 3.3 Total number of CaMKIIα puncta whthin every 50 μm dendritic segment did not change over one hour after group I mGluR stimulation.

The number of CaMKIIα mRNA particles in 50μm dendrite segments was calculated in WT and *fmr1* KO neurons transfected with pIRES-EGFP-mRFP (a), pIRES-EGFP-mRFP-iso1 (b), pIRES-EGFP-mRFP-iso7 (c), or pIRES-EGFP-mRFP-iso2 (d), before or at different time points after 5 min DHPG treatment. There is no difference in the number of total RNA puncta among groups. Data were analyzed from at least 18 dendrites in each group from three independent experiments. Data were analyzed by two-way ANOVA with Tukey-HSD post-test.

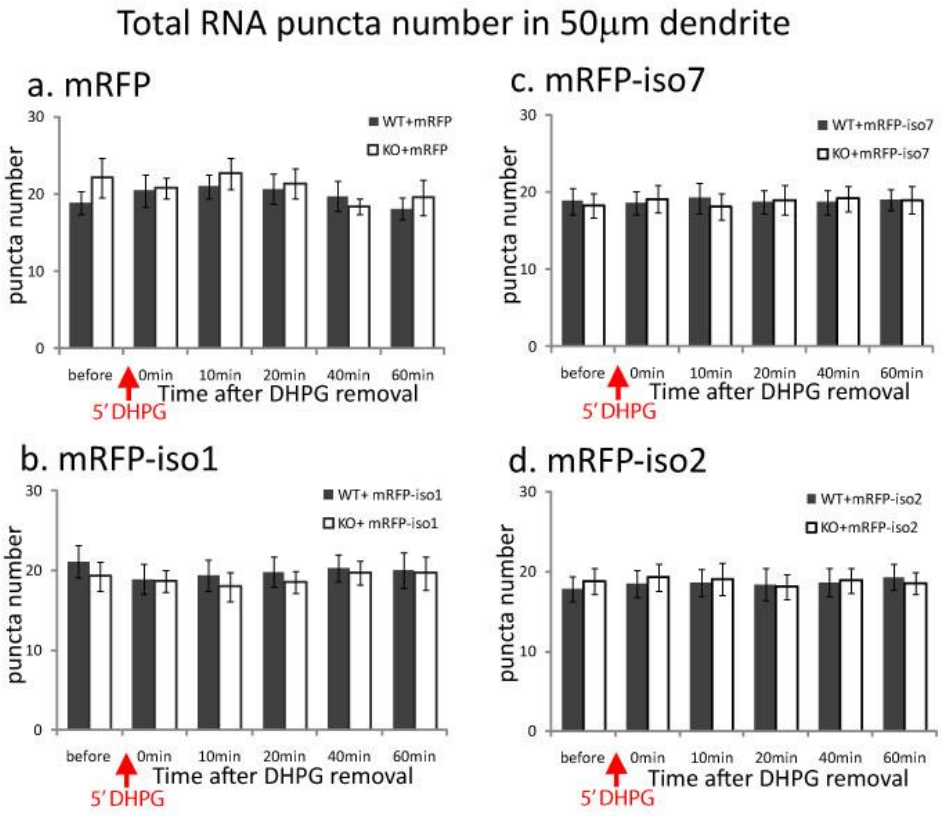

Figure 3.4 Spine localization of endogenous CaMKIIα in *fmr1* KO neurons was not restored by a single FMRP isoform tested here.

The fraction of the number of CaMKIIα mRNA localized in spines versus total number of CaMKIIα in each 50μm dendrite segment was calculated in each group. The data showed a peak fraction after DHPG stimulation in WT but not KO transfected with pIRES-EGFP-mRFP as a control (a), pIRES-EGFP-mRFP-iso1 (b), pIRES-EGFP-mRFP-iso7 (c), or pIRES-EGFP-mRFP-iso2 (d). Data were analyzed from at least 18 dendrites in each group from three independent experiments. The value of ratio was transformed to meet normality requirement and then analyzed by two-way ANOVA with Tukey-HSD. Error bars denote SEM.

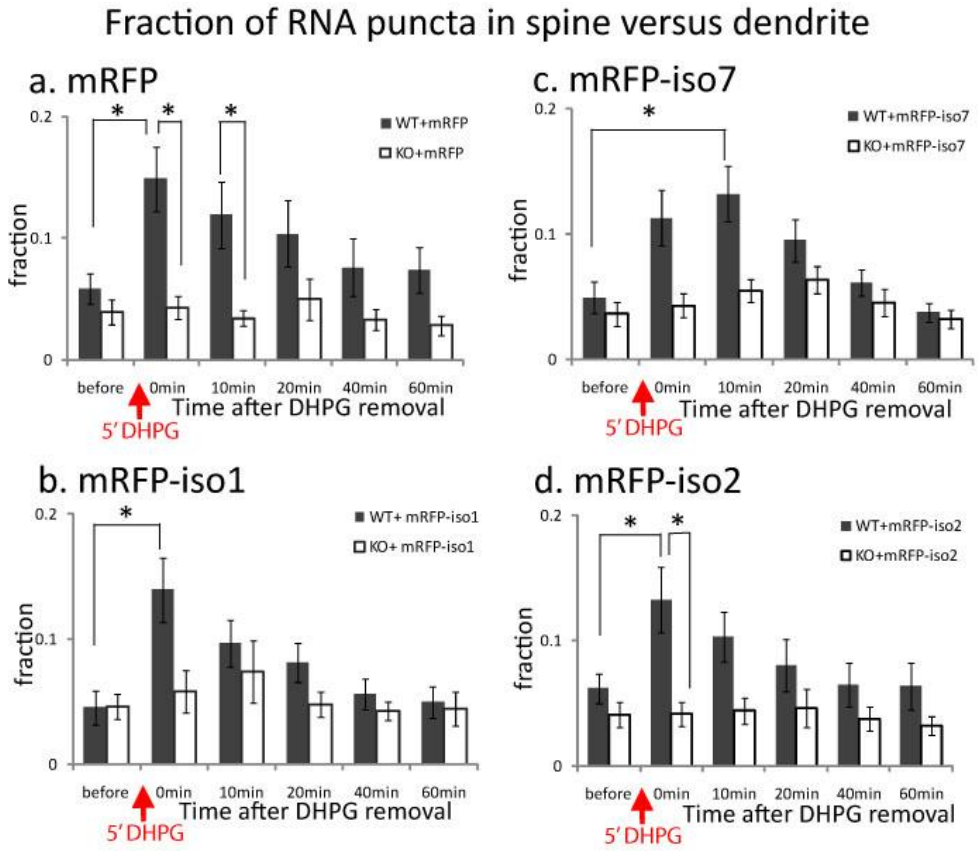

Figure 3.5 Kinetics of isoform by FRAP

FRAP was measured as percentage recovery after photobleaching, 100% as intensity before photobleaching and 0% as intensity after bleaching. Mobile fraction (%) is the percentage of recovery at steady state. Before stimulation (control), iso1 and iso7 had higher mobile fraction (a, b). In response to DHPG, more iso2 and iso8 became mobilized from immobile pools (b, d). Bar graph represents data from three independent experiments, at least 6 dendrites in each experiment. Statistical analysis by independent t-test. Error bars denote SEM.

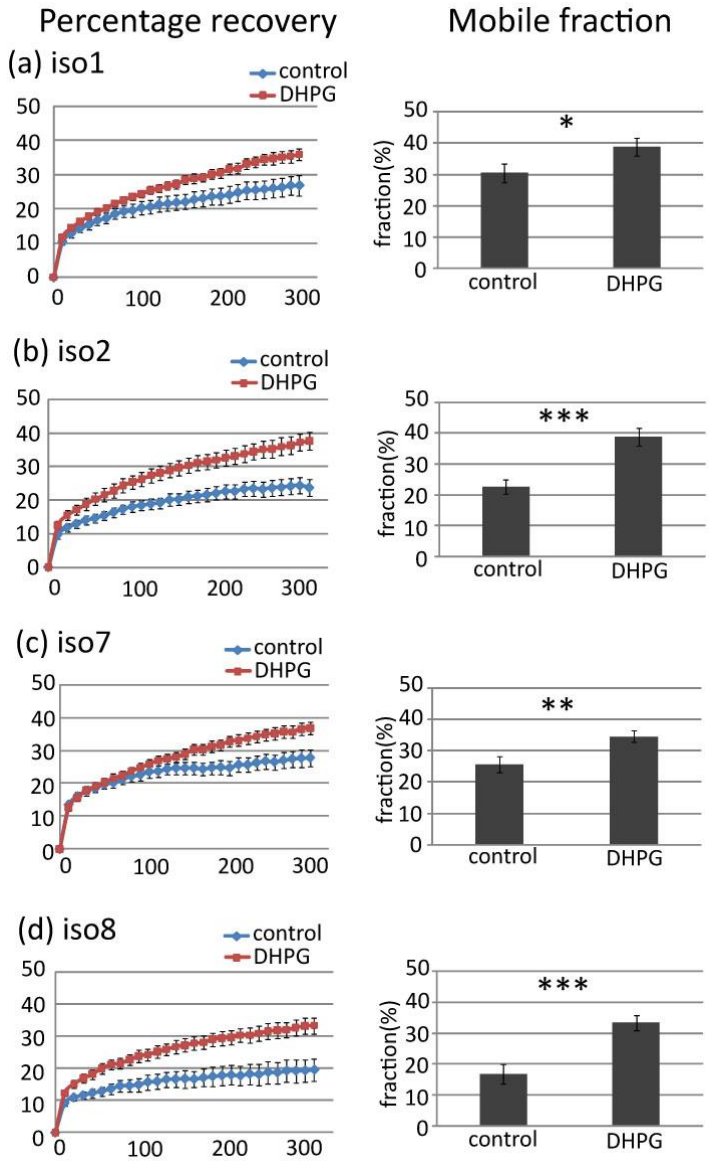

Figure 3.6 Directionality of FMRP isoforms

(a) In WT neurons, iso1 became oscillating at 0-20 minutes after DHPG treatment. (b, c) In only WT neurons, iso2 and iso7 also became more oscillating at 0-20 minutes upon DHPG stimulation. (d) Iso8 does not alter its directionality in response to DHPG. Bar graph represents data from at least three independent experiments, total of at least 40 mRNA particles in each group. Statistical analysis by two-way ANOVA with Tukey HSD post test. Error bars denote SEM.

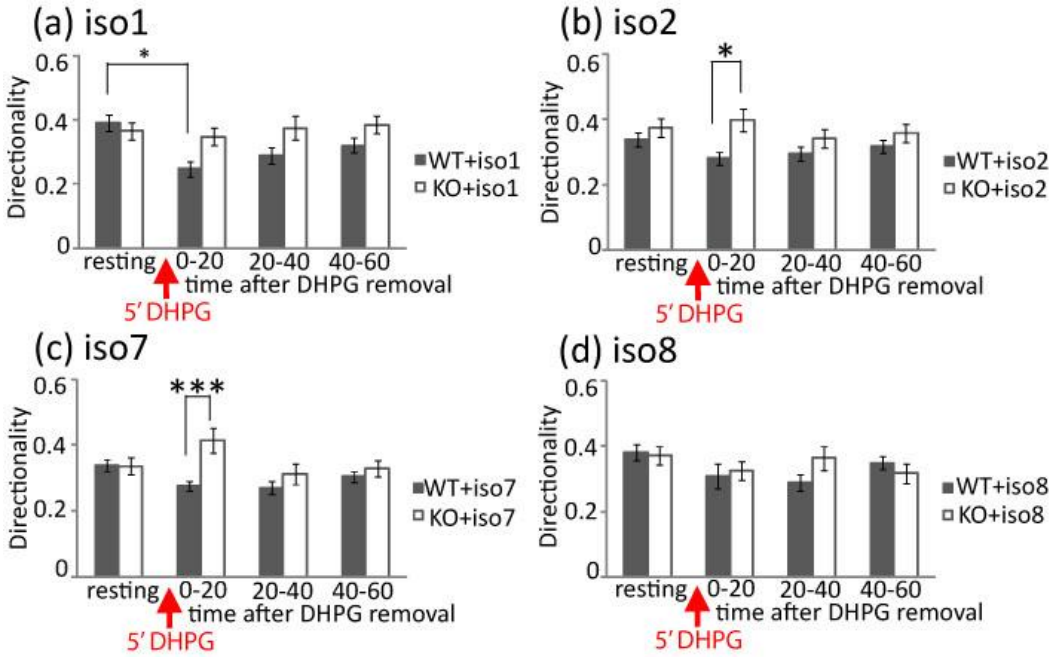

Chapter 4.

Conclusions

My data suggest that FMRP could mediate deceleration of its associated mRNA, along with delivery to dendritic spines for local protein synthesis in response to group I mGluR stimulation. Synaptic mRNA delivery required the presence of more than one FMRP splicing isoform to accomplish the task. The work significantly demonstrated that FMRP as an RNA binding protein is involved in the mechanism of synaptic mRNA delivery.

Synaptic targeting of mRNAs is a critical step to provide materials for local protein synthesis in response to stimulation with temporal and spatial accuracy. With the newly synthesized proteins, spine structure and synaptic connection strength can be modified in the activated synapse. Among about 10,000 synapses in one neuron, the mechanism of local mRNA delivery and protein synthesis is the basis for needed spatial specificity. On the other hand, if local protein synthesis is dysregulated, synapse connection would be abnormally altered, which could cause neurological phenotypes, such as seizures, hyperactivity and mental retardation shown in Fragile X syndrome. Therefore, it is very important to understand the molecular mechanism underlying synaptic mRNA delivery and protein synthesis.

Although alternative splicing of *Fmr1* was reported in 1993 [82], the functional roles of various FMRP splicing isoforms have rarely been studied. To understand the possibility for gene therapy in Fragile X Syndrome, I have used this tool to explore the synaptic mRNA delivery activity of four FMRP isoforms. Phosphorylation modification of FMRP is apparently critical to regulate its synaptic docking. However, it will still require the presence of more than one FMRP isoform to deliver CaMKIIα mRNA to dendritic spines in response to group I mGluR stimulation. This is perhaps not surprising because one synaptic mRNA delivery process would require several events, such as sensing signals, determining directionality, association with motor proteins, mRNAs and even scaffolding proteins, for anchorage and deposition. And the subsequent translation control will also require multiple activities to govern translation initiation or elongation. The diverse functions of FMRP isoforms will be important to be elucidated.

In conclusion, during my PhD studies, my data suggested that FMRP could mediate mRNA synaptic delivery for local protein synthesis, which is likely critical to establish and maintain synaptic connections between neurons. And more than one FMRP splicing isoform would be likely to be involved in the mechanism of synaptic mRNA delivery. The molecular regulation underlying synaptic mRNA delivery for local protein synthesis still needs to be further investigated.

Appendix A.

Lithium treatment of *fmr1* KO mouse model for Fragile X Syndrome

Abstract

To examine the anxiolytic effect of lithium administration in *fmr1* KO mice, marble burying behavior was examined. The *fmr1* KO mouse model is present on two background strains, FVB and C57BL/6. In the FVB strain, lithium reduced the number of buried marbles suggesting that lithium has a general anxiolytic effect in FVB. In untreated C57BL/6, *fmr1* KO buried more marbles than WT. After lithium treatment the number of marbles buried by *fmr1* KO mice was significantly reduced to the level of WT. Therefore, lithium reversed digging/perseverative behavior in C57BL/6 KO. The assay also suggests that the interaction of genetic background and pharmaceutical action could affect behavior outcome.

Introduction

Lithium has been used as a mood stabilizer. It is an FDA approved drug to treat bipolar disorder, depression and other mood disorders. The molecular mechanism underlying lithium treatment is possibly due to its activity in inositol depletion and GSK3β (glycogen synthase kinase-3β) inhibition [127-129]. It is able to suppress manic-depressive episodes and relieve anxiety in bipolar disorder.

Lithium was shown to improve short term memory in courtship conditioning and spine structure deficits in mushroom body in the *Drosophila* model of Fragile X syndrome [130]. However, *dFMR1* gene composition is more similar to mammalian *FXR2*, which is one of two autosomal paralogs of *FMR1*. More recent research in human patients supports the usage of lithium in Fragile X Syndrome. Berry-Kravis et al. demonstrated that in Fragile X Syndrome patients, lithium treatment could improve the score of

patients on Aberrant Behavior Checklist (an assessment of behavior features among mentally retarded individuals) and ERK activation speed to the levels comparable to control patient group [131]. The study encourages future investigation of the molecular mechanism of lithium action in Fragile X Syndrome.

Several promising studies of the mechanism of lithium in the *fmr1* KO mouse model have been published recently. The activity of GSK3β, one target of lithium, is elevated in several brain regions of *fmr1* KO mice. Lithium reduced GSK3b activity and behavioral hyperactivity levels (measured by open field center entry behavior and audiogenic seizures) in *fmr1* KO animals [132]. *Fmr1* KO mice displayed altered anxiety level (by elevated plus-maze test) and fear motivated memory (by passive avoidance test) and impaired social interaction, and these differences were ameliorated by chronic lithium treatment [133-135]. Lithium administration partially normalized longer and increased density of dendritic spine morphology in *fmr1* KO medial prefrontal cortex [133]. These positive effects of lithium treatment in Fragile X animal model support further study in human patients.

In addition to cognition impairment, Fragile X syndrome patients are also at risk for social anxiety [136]. Previously, elevated social anxiety and impaired social interaction in *fmr1* KO mice were shown in social novelty test [137]. Marble burying has been a convenient test to identify anxiolytics. After treatment with anxiolytics, rodents dig/bury fewer marbles. The reason that rodents alter their digging behavior is still unknown. Marbles are not aversive because mice did not avoid the marble-containing side of a two-compartment box [138]. Long term studies suggest that inhibition of marble burying can be used as a correlational model for detection of anxiolytics rather than an isomorphic model of anxiety [138]. Here, a marble burying test was utilized as an assay system to evaluate the lithium effect on anxiety amelioration.

Materials and Methods

Marble burying.

Clean cages (23x44x15 cm) were filled with 4.5cm corncob bedding, on which 20 dark blue glass marbles (15mm diameter) were placed (*Fig. A.1.a*). Three months old mice were habituated for 30 minutes in the behavior room before starting the experiments. One animal was placed in each cage and allowed 30 minutes for exploration. After 30 minutes, the number of marbles buried (to 1/2 surface area) with bedding was counted (*Fig. A.1.b*).

Chronic lithium administration.

Fmr1 KO and WT male mice of FVB and C57BL/6 strains were used. The animals were bred at the Beckman Institute at the University of Illinois-Urbana-Champaign. Following weaning at day 21, mice were housed in same-sex littermate groups in standard laboratory cages with a 12 hour light/dark cycle. Food and water were available *ad libitum*. Mice were divided into four groups as WT, WT treated with lithium, KO, and KO treated with lithium. Mice had unlimited access to regular chow or chow containing 0.24% lithium carbonate (Harlan Teklad, Madison, WI, diet no. 92271) with supplemental saline (0.9%), beginning from two months old till three months old for tests. Measurement of mice serum lithium level was kindly performed by Provena Medical Center, Urbana, IL. Serum lithium level was maintained at 0.73 mmol/L in FVB strain and at 0.5 mmol/L in C57BL/6 strain, which are comparable to standard level in human patients (0.6~ 1.2 mmol/L). Experimental procedures were approved by the Institutional Animal Care and Use Committee at UIUC.

Results

To investigate anxiolytic effect of lithium administration in *fmr1* KO animals, marble burying behavior was examined in WT and *fmr1* KO mice after lithium treatment. Two available mouse strains, FVB and C57BL/6, were both tested because distinct genetic background could account for behavioral differences [139]. Mice in the lithium group

started receiving 0.24% lithium carbonate mixed in regular chow when two months old; after one month of chronic lithium administration, serum lithium level and the marble burying behavior were examined. To avoid lithium toxicity, serum lithium levels were measured and appeared slightly different in two mouse strain: 0.73 mmol/L in FVB and 0.5 mmol/L in C57BL/6. This suggests that the genetic background does affect how lithium is metabolized and maintained in animals. And both lithium levels were comparable to standard level in human patients (0.6~1.2 mmol/L).

In the FVB strain, there is no significant difference between WT and KO genotypes (*Fig. A.2.a*). However, there is a significant effect of lithium treatment (10.1±0.6 marbles in control group and 8.2±0.6 marbles in lithium group, $p<0.05$). Therefore, lithium has a general anxiolytic effect in FVB.

In C57BL/6 (*Fig. A.2.b*), WT and KO exhibited different marble burying behavior in response to lithium (interaction, $p<0.05$). In the control group, KO exhibited significantly higher marble burying activity than WT (10.3±0.9 marbles in control KO group versus 6.1±1.2 marbles in control WT group, $p<0.05$). After lithium treatment, WT persisted in a similar level of burying behavior (5.5±1.0 marbles in lithium treated WT group). But in C57BL/6 KO, the number of buried marbles was significantly reduced after chronic lithium treatment (4.3±1.5 marbles in lithium treated KO group, $p<0.05$). These results suggest that chronic lithium treatment is able to decrease marble burying behavior, as an assessment of anxiolytics, in C57BL/6 *fmr1* KO.

Discussion

We concluded that lithium can relieve anxiety in *fmr1* KO of C57BL/6 but not in FVB by using the marble burying test to assess the anxiolytic effect of lithium. Interestingly, there is elevated level of marble burying behavior in *fmr1* KO of only C57BL/6 background, but not in FVB background. It suggests that the interaction of genetic background and chronic lithium treatment results in different effects in marble burying test. It has been previously reported that different mouse genetic backgrounds indeed influence various

behavior tests [139]. The results are applicable to human patients, in that human populations with different genetic backgrounds may require different pharmaceutical treatment.

Anxiety was measured in *fmr1* KO mice using the elevated plus maze but the results were controversial. In some reports, *fmr1* KO performed as well as WT animals in elevated plus maze [140, 141]. But in others, *fmr1* KO performed poorly in elevated plus maze and the performance could be restored by several drugs [133, 135, 142]. The discrepancy could be caused by the difference in experiment designs but not strain difference. Therefore, our data here could provide another assessment of anxiety deficit and possible anxiolytics in Fragile X Syndrome model.

Although marble burying test has been widely utilized as a model for anxiety or obsessive compulsive disorder (OCD), its physiological relevance is still controversial. Compounds antagonizing serotonin (5-HT) or mGluR5 system, many of which attenuate anxiety, depression or OCD, also inhibited marble burying [143-146]. Since then marble burying has been used as a standard test for anxiety and depression drug discovery. However, Deacon et al. suggested that the marble burying test may best be considered as a species typical behavior that is responsive to many factors since many agents, even psychostimulants, inhibit marble burying behavior [147]. In recent research by Thomas and Paylor et al, it was found that mouse marble burying is not correlated with other anxiety-like traits, not stimulated by novelty, but a repetitive behavior that persists/perseveres with little change across multiple exposures. They also suggested that marble burying is related to repetitive digging behavior and may in fact be more appropriately considered as an indicative measure of perseverative behavior [148]. For future studies in the lab, we should consider marble burying test as a measurement of repetitive digging, which also responds to anxiolytics.

Polyuria (increased urine production) is the most prominent side effect in lithium treated human patients. We observed the same effect in mice. Therefore, mouse bedding was

always changed twice a week in contrast to once per week before treatment. We did not observe other side effects of lithium over-dosage, such as diarrhea, seizures and coma, in mice.

Figures

Figure A.1 Marble burying test apparatus

(a) 20 marbles were spaced evenly in a cage filled with corncob bedding before the test. (b) After 30 minutes exploration, marbles were buried or moved by the mouse. The number of buried marbles was recorded.

a. **b.**

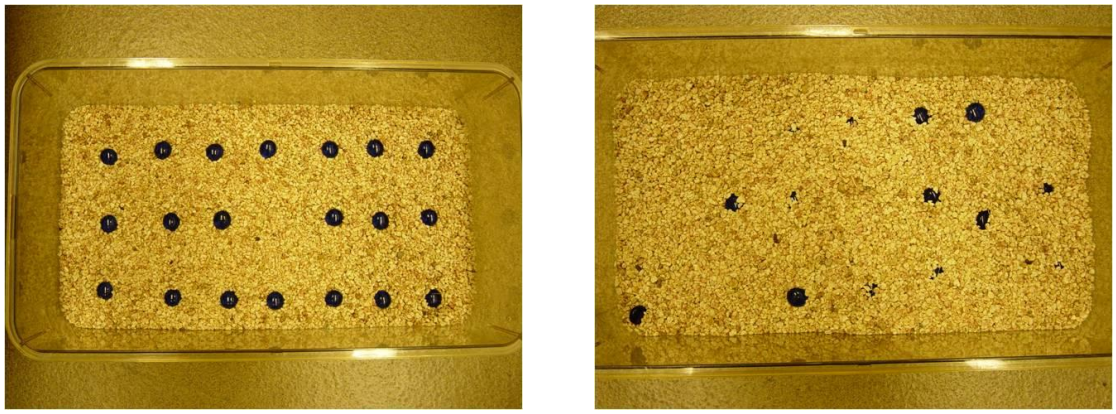

Figure A.2 Effect of administration of lithium on the marble-burying behavior in (a) FVB and (b) C57BL/6 mice.

Each column represents mean± S.E.M. of number of marbles buried in each group. The number of mice in each group is labeled on each column.

a. **b.**

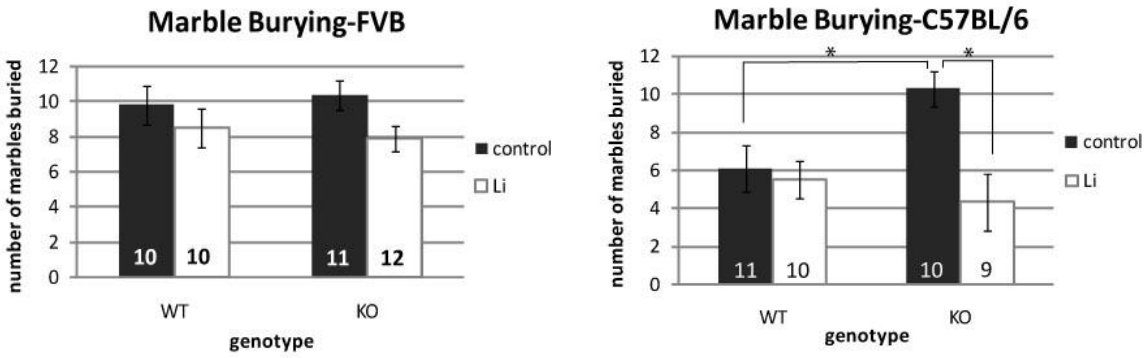

References

1. Sutcliffe, J.S., et al., *DNA methylation represses FMR-1 transcription in fragile X syndrome.* Hum Mol Genet, 1992. **1**(6): p. 397-400.
2. Hagerman, R.J., *Lessons from fragile X regarding neurobiology, autism, and neurodegeneration.* J Dev Behav Pediatr, 2006. **27**(1): p. 63-74.
3. Fu, Y.H., et al., *Variation of the CGG repeat at the fragile X site results in genetic instability: resolution of the Sherman paradox.* Cell, 1991. **67**(6): p. 1047-58.
4. Pieretti, M., et al., *Absence of expression of the FMR-1 gene in fragile X syndrome.* Cell, 1991. **66**(4): p. 817-22.
5. Verkerk, A.J., et al., *Identification of a gene (FMR-1) containing a CGG repeat coincident with a breakpoint cluster region exhibiting length variation in fragile X syndrome.* Cell, 1991. **65**(5): p. 905-14.
6. Hinds, H.L., et al., *Tissue specific expression of FMR-1 provides evidence for a functional role in fragile X syndrome.* Nat Genet, 1993. **3**(1): p. 36-43.
7. *Fmr1 knockout mice: a model to study fragile X mental retardation. The Dutch-Belgian Fragile X Consortium.* Cell, 1994. **78**(1): p. 23-33.
8. Irwin, S.A., R. Galvez, and W.T. Greenough, *Dendritic spine structural anomalies in fragile-X mental retardation syndrome.* Cereb Cortex, 2000. **10**(10): p. 1038-44.
9. Fiala, J.C., J. Spacek, and K.M. Harris, *Dendritic spine pathology: cause or consequence of neurological disorders?* Brain Res Brain Res Rev, 2002. **39**(1): p. 29-54.
10. Huber, K.M., et al., *Altered synaptic plasticity in a mouse model of fragile X mental retardation.* Proc Natl Acad Sci U S A, 2002. **99**(11): p. 7746-50.
11. Steward, O. and E.M. Schuman, *Protein synthesis at synaptic sites on dendrites.* Annu Rev Neurosci, 2001. **24**: p. 299-325.
12. Weiler, I.J., et al., *Fragile X mental retardation protein is translated near synapses in response to neurotransmitter activation.* Proc Natl Acad Sci U S A, 1997. **94**(10): p. 5395-400.
13. Kang, H. and E.M. Schuman, *A requirement for local protein synthesis in neurotrophin-induced hippocampal synaptic plasticity.* Science, 1996. **273**(5280): p. 1402-6.
14. Nosyreva, E.D. and K.M. Huber, *Metabotropic receptor-dependent long-term depression persists in the absence of protein synthesis in the mouse model of fragile X syndrome.* J Neurophysiol, 2006. **95**(5): p. 3291-5.
15. Hernandez, P.J., K. Sadeghian, and A.E. Kelley, *Early consolidation of instrumental learning requires protein synthesis in the nucleus accumbens.* Nat Neurosci, 2002. **5**(12): p. 1327-31.
16. Luft, A.R., et al., *Protein synthesis inhibition blocks consolidation of an acrobatic motor skill.* Learn Mem, 2004. **11**(4): p. 379-82.
17. Miller, S., et al., *Disruption of dendritic translation of CaMKIIalpha impairs stabilization of synaptic plasticity and memory consolidation.* Neuron, 2002. **36**(3): p. 507-19.

18. Vanderklish, P.W. and G.M. Edelman, *Dendritic spines elongate after stimulation of group 1 metabotropic glutamate receptors in cultured hippocampal neurons.* Proc Natl Acad Sci U S A, 2002. **99**(3): p. 1639-44.
19. Bramham, C.R. and D.G. Wells, *Dendritic mRNA: transport, translation and function.* Nat Rev Neurosci, 2007. **8**(10): p. 776-89.
20. Steward, O., et al., *Protein synthesis and processing in cytoplasmic microdomains beneath postsynaptic sites on CNS neurons. A mechanism for establishing and maintaining a mosaic postsynaptic receptive surface.* Mol Neurobiol, 1988. **2**(4): p. 227-61.
21. Steward, O. and E.M. Schuman, *Compartmentalized synthesis and degradation of proteins in neurons.* Neuron, 2003. **40**(2): p. 347-59.
22. Steward, O. and P.M. Falk, *Protein-synthetic machinery at postsynaptic sites during synaptogenesis: a quantitative study of the association between polyribosomes and developing synapses.* J Neurosci, 1986. **6**(2): p. 412-23.
23. Khludova, G.G., *Studies of the relationship between ultrastructural synaptic plasticity and ribosome number in dendritic terminals in the rat neocortex in a cellular conditioning model.* Neurosci Behav Physiol, 1999. **29**(2): p. 175-80.
24. Ostroff, L.E., et al., *Polyribosomes redistribute from dendritic shafts into spines with enlarged synapses during LTP in developing rat hippocampal slices.* Neuron, 2002. **35**(3): p. 535-45.
25. Garner, C.C., R.P. Tucker, and A. Matus, *Selective localization of messenger RNA for cytoskeletal protein MAP2 in dendrites.* Nature, 1988. **336**(6200): p. 674-7.
26. Burgin, K.E., et al., *In situ hybridization histochemistry of Ca2+/calmodulin-dependent protein kinase in developing rat brain.* J Neurosci, 1990. **10**(6): p. 1788-98.
27. Lyford, G.L., et al., *Arc, a growth factor and activity-regulated gene, encodes a novel cytoskeleton-associated protein that is enriched in neuronal dendrites.* Neuron, 1995. **14**(2): p. 433-45.
28. Scheetz, A.J., A.C. Nairn, and M. Constantine-Paton, *NMDA receptor-mediated control of protein synthesis at developing synapses.* Nat Neurosci, 2000. **3**(3): p. 211-6.
29. Kosik, K.S. and A.M. Krichevsky, *The message and the messenger: delivering RNA in neurons.* Sci STKE, 2002. **2002**(126): p. pe16.
30. Torre, E.R. and O. Steward, *Demonstration of local protein synthesis within dendrites using a new cell culture system that permits the isolation of living axons and dendrites from their cell bodies.* J Neurosci, 1992. **12**(3): p. 762-72.
31. Aakalu, G., et al., *Dynamic visualization of local protein synthesis in hippocampal neurons.* Neuron, 2001. **30**(2): p. 489-502.
32. Job, C. and J. Eberwine, *Identification of sites for exponential translation in living dendrites.* Proc Natl Acad Sci U S A, 2001. **98**(23): p. 13037-42.
33. Krichevsky, A.M. and K.S. Kosik, *Neuronal RNA granules: a link between RNA localization and stimulation-dependent translation.* Neuron, 2001. **32**(4): p. 683-96.
34. Wilhelm, J.E., R.D. Vale, and R.S. Hegde, *Coordinate control of translation and localization of Vg1 mRNA in Xenopus oocytes.* Proc Natl Acad Sci U S A, 2000. **97**(24): p. 13132-7.

35. Gavis, E.R. and R. Lehmann, *Translational regulation of nanos by RNA localization.* Nature, 1994. **369**(6478): p. 315-8.
36. Sossin, W.S. and L. DesGroseillers, *Intracellular trafficking of RNA in neurons.* Traffic, 2006. **7**(12): p. 1581-9.
37. Kiebler, M.A. and G.J. Bassell, *Neuronal RNA granules: movers and makers.* Neuron, 2006. **51**(6): p. 685-90.
38. Bell, T.J., et al., *Cytoplasmic BK(Ca) channel intron-containing mRNAs contribute to the intrinsic excitability of hippocampal neurons.* Proc Natl Acad Sci U S A, 2008. **105**(6): p. 1901-6.
39. Glanzer, J., et al., *RNA splicing capability of live neuronal dendrites.* Proc Natl Acad Sci U S A, 2005. **102**(46): p. 16859-64.
40. Giorgi, C., et al., *The EJC factor eIF4AIII modulates synaptic strength and neuronal protein expression.* Cell, 2007. **130**(1): p. 179-91.
41. Ceman, S., et al., *Phosphorylation influences the translation state of FMRP-associated polyribosomes.* Hum Mol Genet, 2003. **12**(24): p. 3295-305.
42. Kanai, Y., N. Dohmae, and N. Hirokawa, *Kinesin transports RNA: isolation and characterization of an RNA-transporting granule.* Neuron, 2004. **43**(4): p. 513-25.
43. Elvira, G., et al., *Characterization of an RNA granule from developing brain.* Mol Cell Proteomics, 2006. **5**(4): p. 635-51.
44. Steward, O., et al., *Synaptic activation causes the mRNA for the IEG Arc to localize selectively near activated postsynaptic sites on dendrites.* Neuron, 1998. **21**(4): p. 741-51.
45. Steward, O. and P.F. Worley, *Selective targeting of newly synthesized Arc mRNA to active synapses requires NMDA receptor activation.* Neuron, 2001. **30**(1): p. 227-40.
46. Huang, F., J.K. Chotiner, and O. Steward, *Actin polymerization and ERK phosphorylation are required for Arc/Arg3.1 mRNA targeting to activated synaptic sites on dendrites.* J Neurosci, 2007. **27**(34): p. 9054-67.
47. Yoshimura, A., et al., *Myosin-Va facilitates the accumulation of mRNA/protein complex in dendritic spines.* Curr Biol, 2006. **16**(23): p. 2345-51.
48. Ferrari, F., et al., *The fragile X mental retardation protein-RNP granules show an mGluR-dependent localization in the post-synaptic spines.* Mol Cell Neurosci, 2007. **34**(3): p. 343-54.
49. Bourne, J.N., et al., *Polyribosomes are increased in spines of CA1 dendrites 2 h after the induction of LTP in mature rat hippocampal slices.* Hippocampus, 2007. **17**(1): p. 1-4.
50. Steward, O. and W.B. Levy, *Preferential localization of polyribosomes under the base of dendritic spines in granule cells of the dentate gyrus.* J Neurosci, 1982. **2**(3): p. 284-91.
51. Ashley, C.T., Jr., et al., *FMR1 protein: conserved RNP family domains and selective RNA binding.* Science, 1993. **262**(5133): p. 563-6.
52. Tamanini, F., et al., *FMRP is associated to the ribosomes via RNA.* Hum Mol Genet, 1996. **5**(6): p. 809-13.
53. Miyashiro, K.Y., et al., *RNA cargoes associating with FMRP reveal deficits in cellular functioning in Fmr1 null mice.* Neuron, 2003. **37**(3): p. 417-31.

54. Brown, V., et al., *Microarray identification of FMRP-associated brain mRNAs and altered mRNA translational profiles in fragile X syndrome.* Cell, 2001. **107**(4): p. 477-87.
55. Hou, L., et al., *Dynamic translational and proteasomal regulation of fragile X mental retardation protein controls mGluR-dependent long-term depression.* Neuron, 2006. **51**(4): p. 441-54.
56. Todd, P.K., K.J. Mack, and J.S. Malter, *The fragile X mental retardation protein is required for type-I metabotropic glutamate receptor-dependent translation of PSD-95.* Proc Natl Acad Sci U S A, 2003. **100**(24): p. 14374-8.
57. Lu, R., et al., *The fragile X protein controls microtubule-associated protein 1B translation and microtubule stability in brain neuron development.* Proc Natl Acad Sci U S A, 2004. **101**(42): p. 15201-6.
58. Nakamoto, M., et al., *Fragile X mental retardation protein deficiency leads to excessive mGluR5-dependent internalization of AMPA receptors.* Proc Natl Acad Sci U S A, 2007. **104**(39): p. 15537-42.
59. Volk, L.J., et al., *Multiple Gq-coupled receptors converge on a common protein synthesis-dependent long-term depression that is affected in fragile X syndrome mental retardation.* J Neurosci, 2007. **27**(43): p. 11624-34.
60. Ling, S.C., et al., *Transport of Drosophila fragile X mental retardation protein-containing ribonucleoprotein granules by kinesin-1 and cytoplasmic dynein.* Proc Natl Acad Sci U S A, 2004. **101**(50): p. 17428-33.
61. Davidovic, L., et al., *The fragile X mental retardation protein is a molecular adaptor between the neurospecific KIF3C kinesin and dendritic RNA granules.* Hum Mol Genet, 2007. **16**(24): p. 3047-58.
62. Wang, H., et al., *Dynamic association of the fragile X mental retardation protein as a messenger ribonucleoprotein between microtubules and polyribosomes.* Mol Biol Cell, 2008. **19**(1): p. 105-14.
63. Antar, L.N., et al., *Metabotropic glutamate receptor activation regulates fragile x mental retardation protein and FMR1 mRNA localization differentially in dendrites and at synapses.* J Neurosci, 2004. **24**(11): p. 2648-55.
64. Muddashetty, R.S., et al., *Dysregulated metabotropic glutamate receptor-dependent translation of AMPA receptor and postsynaptic density-95 mRNAs at synapses in a mouse model of fragile X syndrome.* J Neurosci, 2007. **27**(20): p. 5338-48.
65. Dictenberg, J.B., et al., *A direct role for FMRP in activity-dependent dendritic mRNA transport links filopodial-spine morphogenesis to fragile X syndrome.* Dev Cell, 2008. **14**(6): p. 926-39.
66. Greenough, W.T., et al., *Synaptic regulation of protein synthesis and the fragile X protein.* Proc Natl Acad Sci U S A, 2001. **98**(13): p. 7101-6.
67. Khandjian, E.W., *Biology of the fragile X mental retardation protein, an RNA-binding protein.* Biochem Cell Biol, 1999. **77**(4): p. 331-42.
68. Annangudi, S.P., et al., *Neuropeptide Release is Impaired in a Mouse Model of Fragile X Mental Retardation Syndrome.* ACS Chem Neurosci, 2010. **1**(4): p. 306-314.

69. Li, C., G.J. Bassell, and Y. Sasaki, *Fragile X Mental Retardation Protein is Involved in Protein Synthesis-Dependent Collapse of Growth Cones Induced by Semaphorin-3A.* Front Neural Circuits, 2009. **3**: p. 11.
70. Menon, L. and M.R. Mihailescu, *Interactions of the G quartet forming semaphorin 3F RNA with the RGG box domain of the fragile X protein family.* Nucleic Acids Res, 2007. **35**(16): p. 5379-92.
71. Fernandez de Sevilla, D. and W. Buno, *The muscarinic long-term enhancement of NMDA and AMPA receptor-mediated transmission at Schaffer collateral synapses develop through different intracellular mechanisms.* J Neurosci. **30**(33): p. 11032-42.
72. Silva, A.J., et al., *Deficient hippocampal long-term potentiation in alpha-calcium-calmodulin kinase II mutant mice.* Science, 1992. **257**(5067): p. 201-6.
73. Ouyang, Y., et al., *Visualization of the distribution of autophosphorylated calcium/calmodulin-dependent protein kinase II after tetanic stimulation in the CA1 area of the hippocampus.* J Neurosci, 1997. **17**(14): p. 5416-27.
74. Hansel, C., et al., *alphaCaMKII Is essential for cerebellar LTD and motor learning.* Neuron, 2006. **51**(6): p. 835-43.
75. Mayford, M., et al., *CaMKII regulates the frequency-response function of hippocampal synapses for the production of both LTD and LTP.* Cell, 1995. **81**(6): p. 891-904.
76. El-Husseini, A.E., et al., *PSD-95 involvement in maturation of excitatory synapses.* Science, 2000. **290**(5495): p. 1364-8.
77. Gonzalez-Billault, C., et al., *Microtubule-associated protein 1B function during normal development, regeneration, and pathological conditions in the nervous system.* J Neurobiol, 2004. **58**(1): p. 48-59.
78. Davidkova, G. and R.C. Carroll, *Characterization of the role of microtubule-associated protein 1B in metabotropic glutamate receptor-mediated endocytosis of AMPA receptors in hippocampus.* J Neurosci, 2007. **27**(48): p. 13273-8.
79. Menon, L., S.A. Mader, and M.R. Mihailescu, *Fragile X mental retardation protein interactions with the microtubule associated protein 1B RNA.* Rna, 2008. **14**(8): p. 1644-55.
80. Verkerk, A.J., et al., *Alternative splicing in the fragile X gene FMR1.* Hum Mol Genet, 1993. **2**(4): p. 399-404.
81. Eichler, E.E., et al., *Fine structure of the human FMR1 gene.* Hum Mol Genet, 1993. **2**(8): p. 1147-53.
82. Ashley, C.T., et al., *Human and murine FMR-1: alternative splicing and translational initiation downstream of the CGG-repeat.* Nat Genet, 1993. **4**(3): p. 244-51.
83. Sittler, A., et al., *Alternative splicing of exon 14 determines nuclear or cytoplasmic localisation of fmr1 protein isoforms.* Hum Mol Genet, 1996. **5**(1): p. 95-102.
84. Xie, W., et al., *Tissue and developmental regulation of fragile X mental retardation 1 exon 12 and 15 isoforms.* Neurobiol Dis, 2009. **35**(1): p. 52-62.
85. Dolzhanskaya, N., G. Merz, and R.B. Denman, *Alternative splicing modulates protein arginine methyltransferase-dependent methylation of fragile X syndrome mental retardation protein.* Biochemistry, 2006. **45**(34): p. 10385-93.

86. Denman, R.B. and Y.J. Sung, *Species-specific and isoform-specific RNA binding of human and mouse fragile X mental retardation proteins.* Biochem Biophys Res Commun, 2002. **292**(4): p. 1063-9.
87. Steward, O. and P.F. Worley, *A cellular mechanism for targeting newly synthesized mRNAs to synaptic sites on dendrites.* Proc Natl Acad Sci U S A, 2001. **98**(13): p. 7062-8.
88. Paradies, M.A. and O. Steward, *Multiple subcellular mRNA distribution patterns in neurons: a nonisotopic in situ hybridization analysis.* J Neurobiol, 1997. **33**(4): p. 473-93.
89. Manders, E.E.M., F.J. Verbeek, and J.A. Aten, *Measurement of co-localisation of objects in dual-colour confocal images.* J. Microscopy, 1993. **169**: p. 375-382.
90. Rook, M.S., M. Lu, and K.S. Kosik, *CaMKIIalpha 3' untranslated region-directed mRNA translocation in living neurons: visualization by GFP linkage.* J Neurosci, 2000. **20**(17): p. 6385-93.
91. Bertrand, E., et al., *Localization of ASH1 mRNA particles in living yeast.* Mol Cell, 1998. **2**(4): p. 437-45.
92. Schaeffer, C., et al., *The fragile X mental retardation protein binds specifically to its mRNA via a purine quartet motif.* Embo J, 2001. **20**(17): p. 4803-13.
93. Dolzhanskaya, N., et al., *The fragile X mental retardation protein interacts with U-rich RNAs in a yeast three-hybrid system.* Biochem Biophys Res Commun, 2003. **305**(2): p. 434-41.
94. Burgueno, J., et al., *Metabotropic glutamate type 1alpha receptor localizes in low-density caveolin-rich plasma membrane fractions.* J Neurochem, 2003. **86**(4): p. 785-91.
95. Gallagher, S.M., et al., *Extracellular signal-regulated protein kinase activation is required for metabotropic glutamate receptor-dependent long-term depression in hippocampal area CA1.* J Neurosci, 2004. **24**(20): p. 4859-64.
96. Fujii, R., et al., *The RNA binding protein TLS is translocated to dendritic spines by mGluR5 activation and regulates spine morphology.* Curr Biol, 2005. **15**(6): p. 587-93.
97. Ohashi, S., et al., *Identification of mRNA/protein (mRNP) complexes containing Puralpha, mStaufen, fragile X protein, and myosin Va and their association with rough endoplasmic reticulum equipped with a kinesin motor.* J Biol Chem, 2002. **277**(40): p. 37804-10.
98. Estes, P.S., et al., *Fragile X protein controls the efficacy of mRNA transport in Drosophila neurons.* Mol Cell Neurosci, 2008. **39**(2): p. 170-9.
99. Barbee, S.A., et al., *Staufen- and FMRP-containing neuronal RNPs are structurally and functionally related to somatic P bodies.* Neuron, 2006. **52**(6): p. 997-1009.
100. Zeitelhofer, M., et al., *Dynamic interaction between P-bodies and transport ribonucleoprotein particles in dendrites of mature hippocampal neurons.* J Neurosci, 2008. **28**(30): p. 7555-62.
101. Mazroui, R., et al., *Trapping of messenger RNA by Fragile X Mental Retardation protein into cytoplasmic granules induces translation repression.* Hum Mol Genet, 2002. **11**(24): p. 3007-17.

102. Kim, S.H., et al., *Fragile X mental retardation protein shifts between polyribosomes and stress granules after neuronal injury by arsenite stress or in vivo hippocampal electrode insertion.* J Neurosci, 2006. **26**(9): p. 2413-8.
103. Grossman, A.W., et al., *Local protein synthesis and spine morphogenesis: Fragile X syndrome and beyond.* J Neurosci, 2006. **26**(27): p. 7151-5.
104. Antar, L.N., et al., *Localization of FMRP-associated mRNA granules and requirement of microtubules for activity-dependent trafficking in hippocampal neurons.* Genes Brain Behav, 2005. **4**(6): p. 350-9.
105. Cheever, A. and S. Ceman, *Phosphorylation of FMRP inhibits association with Dicer.* Rna, 2009. **15**(3): p. 362-6.
106. Edbauer, D., et al., *Regulation of synaptic structure and function by FMRP-associated microRNAs miR-125b and miR-132.* Neuron, 2010. **65**(3): p. 373-84.
107. Irwin, S.A., et al., *Fragile X mental retardation protein levels increase following complex environment exposure in rat brain regions undergoing active synaptogenesis.* Neurobiol Learn Mem, 2005. **83**(3): p. 180-7.
108. Zeier, Z., et al., *Fragile X mental retardation protein replacement restores hippocampal synaptic function in a mouse model of fragile X syndrome.* Gene Ther, 2009. **16**(9): p. 1122-9.
109. Pfeiffer, B.E. and K.M. Huber, *Fragile X mental retardation protein induces synapse loss through acute postsynaptic translational regulation.* J Neurosci, 2007. **27**(12): p. 3120-30.
110. Darnell, J.C., et al., *Discrimination of common and unique RNA-binding activities among Fragile X mental retardation protein paralogs.* Hum Mol Genet, 2009. **18**(17): p. 3164-77.
111. Didiot, M.C., et al., *The G-quartet containing FMRP binding site in FMR1 mRNA is a potent exonic splicing enhancer.* Nucleic Acids Res, 2008. **36**(15): p. 4902-12.
112. Lippincott-Schwartz, J., E. Snapp, and A. Kenworthy, *Studying protein dynamics in living cells.* Nat Rev Mol Cell Biol, 2001. **2**(6): p. 444-56.
113. Kao, D.I., et al., *Altered mRNA transport, docking, and protein translation in neurons lacking fragile X mental retardation protein.* Proc Natl Acad Sci U S A, 2010. **107**(35): p. 15601-6.
114. Narayanan, U., et al., *FMRP phosphorylation reveals an immediate-early signaling pathway triggered by group I mGluR and mediated by PP2A.* J Neurosci, 2007. **27**(52): p. 14349-57.
115. Narayanan, U., et al., *S6K1 phosphorylates and regulates fragile X mental retardation protein (FMRP) with the neuronal protein synthesis-dependent mammalian target of rapamycin (mTOR) signaling cascade.* J Biol Chem, 2008. **283**(27): p. 18478-82.
116. Tamanini, F., et al., *Oligomerization properties of fragile-X mental-retardation protein (FMRP) and the fragile-X-related proteins FXR1P and FXR2P.* Biochem J, 1999. **343 Pt 3**: p. 517-23.
117. Bakker, C.E., et al., *Immunocytochemical and biochemical characterization of FMRP, FXR1P, and FXR2P in the mouse.* Exp Cell Res, 2000. **258**(1): p. 162-70.

118. Mientjes, E.J., et al., *Fxr1 knockout mice show a striated muscle phenotype: implications for Fxr1p function in vivo.* Hum Mol Genet, 2004. **13**(13): p. 1291-302.
119. Bontekoe, C.J., et al., *Knockout mouse model for Fxr2: a model for mental retardation.* Hum Mol Genet, 2002. **11**(5): p. 487-98.
120. Spencer, C.M., et al., *Exaggerated behavioral phenotypes in Fmr1/Fxr2 double knockout mice reveal a functional genetic interaction between Fragile X-related proteins.* Hum Mol Genet, 2006. **15**(12): p. 1984-94.
121. Schenck, A., et al., *A highly conserved protein family interacting with the fragile X mental retardation protein (FMRP) and displaying selective interactions with FMRP-related proteins FXR1P and FXR2P.* Proc Natl Acad Sci U S A, 2001. **98**(15): p. 8844-9.
122. Schenck, A., et al., *CYFIP/Sra-1 controls neuronal connectivity in Drosophila and links the Rac1 GTPase pathway to the fragile X protein.* Neuron, 2003. **38**(6): p. 887-98.
123. Bardoni, B., et al., *NUFIP1 (nuclear FMRP interacting protein 1) is a nucleocytoplasmic shuttling protein associated with active synaptoneurosomes.* Exp Cell Res, 2003. **289**(1): p. 95-107.
124. Bardoni, B., et al., *82-FIP, a novel FMRP (fragile X mental retardation protein) interacting protein, shows a cell cycle-dependent intracellular localization.* Hum Mol Genet, 2003. **12**(14): p. 1689-98.
125. Bardoni, B., A. Schenck, and J.L. Mandel, *A novel RNA-binding nuclear protein that interacts with the fragile X mental retardation (FMR1) protein.* Hum Mol Genet, 1999. **8**(13): p. 2557-66.
126. Feng, Y., et al., *FMRP associates with polyribosomes as an mRNP, and the I304N mutation of severe fragile X syndrome abolishes this association.* Mol Cell, 1997. **1**(1): p. 109-18.
127. Beaulieu, J.M., et al., *A beta-arrestin 2 signaling complex mediates lithium action on behavior.* Cell, 2008. **132**(1): p. 125-36.
128. Williams, R.S., et al., *A common mechanism of action for three mood-stabilizing drugs.* Nature, 2002. **417**(6886): p. 292-5.
129. Berridge, M.J., *Unlocking the secrets of cell signaling.* Annu Rev Physiol, 2005. **67**: p. 1-21.
130. McBride, S.M., et al., *Pharmacological rescue of synaptic plasticity, courtship behavior, and mushroom body defects in a Drosophila model of fragile X syndrome.* Neuron, 2005. **45**(5): p. 753-64.
131. Berry-Kravis, E., et al., *Open-label treatment trial of lithium to target the underlying defect in fragile X syndrome.* J Dev Behav Pediatr, 2008. **29**(4): p. 293-302.
132. Min, W.W., et al., *Elevated glycogen synthase kinase-3 activity in Fragile X mice: key metabolic regulator with evidence for treatment potential.* Neuropharmacology, 2009. **56**(2): p. 463-72.
133. Liu, Z.H., D.M. Chuang, and C.B. Smith, *Lithium ameliorates phenotypic deficits in a mouse model of fragile X syndrome.* Int J Neuropsychopharmacol, 2010: p. 1-13.

134. Mines, M.A., et al., *GSK3 influences social preference and anxiety-related behaviors during social interaction in a mouse model of fragile X syndrome and autism.* PLoS One, 2010. **5**(3): p. e9706.
135. Yuskaitis, C.J., et al., *Lithium ameliorates altered glycogen synthase kinase-3 and behavior in a mouse model of fragile X syndrome.* Biochem Pharmacol, 2010. **79**(4): p. 632-46.
136. Hessl, D., et al., *The influence of environmental and genetic factors on behavior problems and autistic symptoms in boys and girls with fragile X syndrome.* Pediatrics, 2001. **108**(5): p. E88.
137. McNaughton, C.H., et al., *Evidence for social anxiety and impaired social cognition in a mouse model of fragile X syndrome.* Behav Neurosci, 2008. **122**(2): p. 293-300.
138. Njung'e, K. and S.L. Handley, *Evaluation of marble-burying behavior as a model of anxiety.* Pharmacol Biochem Behav, 1991. **38**(1): p. 63-7.
139. Crawley, J.N., et al., *Behavioral phenotypes of inbred mouse strains: implications and recommendations for molecular studies.* Psychopharmacology (Berl), 1997. **132**(2): p. 107-24.
140. Mineur, Y.S., et al., *Behavioral and neuroanatomical characterization of the Fmr1 knockout mouse.* Hippocampus, 2002. **12**(1): p. 39-46.
141. Nielsen, D.M., et al., *Alterations in the auditory startle response in Fmr1 targeted mutant mouse models of fragile X syndrome.* Brain Res, 2002. **927**(1): p. 8-17.
142. Bilousova, T.V., et al., *Minocycline promotes dendritic spine maturation and improves behavioural performance in the fragile X mouse model.* J Med Genet, 2009. **46**(2): p. 94-102.
143. Spooren, W.P., et al., *Anxiolytic-like effects of the prototypical metabotropic glutamate receptor 5 antagonist 2-methyl-6-(phenylethynyl)pyridine in rodents.* J Pharmacol Exp Ther, 2000. **295**(3): p. 1267-75.
144. Brodkin, J., et al., *Anxiolytic-like activity of the mGluR5 antagonist MPEP: a comparison with diazepam and buspirone.* Pharmacol Biochem Behav, 2002. **73**(2): p. 359-66.
145. Hirano, K., et al., *Relationship between brain serotonin transporter binding, plasma concentration and behavioural effect of selective serotonin reuptake inhibitors.* Br J Pharmacol, 2005. **144**(5): p. 695-702.
146. Njung'e, K. and S.L. Handley, *Effects of 5-HT uptake inhibitors, agonists and antagonists on the burying of harmless objects by mice; a putative test for anxiolytic agents.* Br J Pharmacol, 1991. **104**(1): p. 105-12.
147. Deacon, R.M., *Digging and marble burying in mice: simple methods for in vivo identification of biological impacts.* Nat Protoc, 2006. **1**(1): p. 122-4.
148. Thomas, A., et al., *Marble burying reflects a repetitive and perseverative behavior more than novelty-induced anxiety.* Psychopharmacology (Berl), 2009. **204**(2): p. 361-73.